Polymer Processing in a Circular Plastic Economy

A thesis submitted to The University of Manchester for the Degree of

Master of Philosophy

in the Faculty of Science and Engineering.

2022

Selin N Palali

School of Natural Sciences/ Department of Materials

Table of Contents

List of Figures

List of Tables

List of Schemes

Abbreviations

ABS – Acrylonitrile Butadiene Styrene

AO – Antioxidant

ATH – Aluminium Trihydrate

ATR – Attenuated Total Reflection

CEP – Circular Economy Package

CI – Carbonyl Index

DRS – Deposit Return Scheme

DSC – Differential Scanning Calorimetry

EPR – Extended Producer Responsibility

FR – Fire Retardant

FTIR – Fourier Transform Infrared Spectroscopy

GHG – Greenhouse Gas Emission

GWP – Global Warming Potential

HALS – Hindered Amine Light Stabiliser

HAS – Hindered Amine Stabiliser

HDPE – High Density Polyethylene

HPLC – High Pressure Liquid Chromatography

LCA – Life-cycle Assessment

LDPE – Low Density Polyethylene

LLDPE – Linear Low Density Polyethylene

MFI – Melt Flow Index

MP – Microplastics

MS – Mass Spectroscopy

MSW – Municipal Solid Waste

Mt – Million Metric Tons

MW – Molecular Weight

MWD – Molecular Weight Distribution

NMR – Nuclear Magnetic Resonance

PBT – Poly (butylene terephthalate)

PET – Polyethylene Terephthalate

pHRR – Peak Heat Release Rate

PMMA – Poly (methyl methacrylate)

PP – Polypropylene

PPE – Personal Protective Equipment

PS – Polystyrene

PVC – Polyvinyl Chloride

RPM – Revolutions per Minute

SEC – Size Exclusion Chromatography

SME – Specific Mechanical Energy

YI – Yellowness Index

YM – Young's Modulus

ZN – Ziegler-Natta

Abstract

With the sharp increase of plastic waste, the current linear global plastic economy is putting strain on industries to adopt to a circular plastic economy. High density polyethylene (HDPE) has one of the largest shares (~ 20 %) in municipal waste streams owing to its favourable properties such as low cost and durability. One approach is to mechanically recycle these plastic resins via extrusion. However, plastics' mechanical properties significantly deteriorate once the material is subject to harsh processing conditions such as high temperatures and shear force. In this project, the relationship between the mechanical, thermal and rheological properties of multiple virgin grades were analysed, and correlations between grade-based properties were confirmed. As such, this research can facilitate the development of a mapping system using a linear regression model to predict the properties of an HDPE grade and its recycling prospects. Additives such as antioxidants can reduce the rate of thermo-oxidative degradation but increase discolouration during recycling. Therefore, the yellowness index between recycling cycles were analysed, and preliminary Soxhlet extraction experiments were carried out to identify additive content and improve extraction parameters. Following this, various HDPE grades were exposed to several recycling cycles and the resulting degradation kinetics were compared and analysed. The highest melt-flow index (MFI) grade displayed increasing Young's Modulus (5.6 %) and tensile strength (3.3 %), but a significant decrease in elongation at break (52 %) when recycled. The change in thermal properties of all grades were little to none. Likewise, nominal changes were seen in the rheological properties of the grades with increased recycling, however, the low MFI grade displayed unusual properties with variations in shear dependent viscosity. Nonetheless, low MFI grades showed better mechanical behaviour, and in general less degradation during recycling resulting from less variation in properties. Overall, a successful foundation of research was developed to understand the relationship between recyclate quality and MFI, and facilitate an efficient circular polymer processing system.

Declaration

No portion of the work referred to in the thesis has been submitted in support of an application for another degree or qualification of this or any other university or other institute of learning

Selin Nur Palali

31/03/2022

Copyright Statement

i. The author of this thesis (including any appendices and/or schedules to this thesis) owns certain copyright or related rights in it (the "Copyright") and she has given the University of Manchester certain rights to use such Copyright, including for administrative purposes.

ii. Copies of this thesis, either in full or in extracts and whether in hard or electronic copy, may be made **only** in accordance with the Copyright, Designs and Patents Act 1988 (as amended) and regulations issued under it or, where appropriate, in accordance with licensing agreements which the University has from time to time. This page must form part of any such copies made.

iii. The ownership of certain Copyright, patents, designs, trademarks and other intellectual property (the "Intellectual Property") and any reproductions of copyright works in the thesis, for example graphs and tables ("Reproductions"), which may be described in this thesis, may not be owned by the author and may be owned by third parties. Such Intellectual Property and Reproductions cannot and must not be made available for use without the prior written permission of the owner(s) of the relevant Intellectual Property and/or Reproductions.

iv. Further information on the conditions under which disclosure, publication and commercialisation of this thesis, the Copyright and any Intellectual Property and/or Reproductions described in it may take place is available in the University IP Policy (see http://documents.manchester.ac.uk/DocuInfo.aspx?DocID=24420), in any relevant Thesis restriction declarations deposited in the University Library, the University Library's regulations (see http://www.library.manchester.ac.uk/about/regulations/) and in the University's policy on Presentation of Theses.

Acknowledgements

I am very grateful for the SMI hub and everyone in the GML group. Firstly, thank you Professor Michael Shaver for always making time, and giving countless individual advice and support. I feel very fortunate to have worked with you. Thank you Zoé Schyns for being an inspirational mentor and helping me along this journey, you are a great scientist and I look forward to seeing the places you'll go. Additionally, thank you Dr. Siobhan Kilbride, Dr. Guilhem De Hoe, and thank you Dr. Christina Picken for your emotional support and motivation, you have a pure heart of gold and have always been by my side. Special thanks to the University of Manchester and Henry Royce Institute for providing wonderful facilities, equipment, and a great research and learning environment.

And finally, thank you to my parents, Fatik and Cuma, and my brother Tahir, for giving me the best education they could afford and making me into the person I am today.

This thesis is dedicated to my family and for the hardships and oppressions they have endured. I wish every child the right to knowledge and education, despite their background, race and privilege.

I look forward to the challenges ahead, and this is only the beginning of my journey in science.

1 Introduction

1.1 The Plastic Demand

Plastics play a key role in modern society and are the backbone of globalisation. Almost all sectors of industry are dependent upon the plastic economy, from pharmaceuticals and healthcare, to food and infrastructure.[1,2,3] Global plastic production is on the rise, and in 2019 reached 370 million metric tonnes (Mt) per annum, surpassing the total biomass of terrestrial and marine animals combined.[4,5,6] If present plastic manufacturing and waste management trends continue, the global waste levels are projected to increase to over 25,000 million Mt per year by 2050 (**Figure 1. 1**), and a total of 12,000 million Mt of plastic waste will be in landfill or the environment.[7,8]

Managing consumer plastics at end-of-life is a challenge. [9,4] Plastics are frequently disposed of after a single use, but due to their durability they have slow degradation rates and persist in the environment. For example, in the terrestrial and marine settings, complete degradation of an HDPE bottle is projected to take 500 and 116 years, respectively.[10]

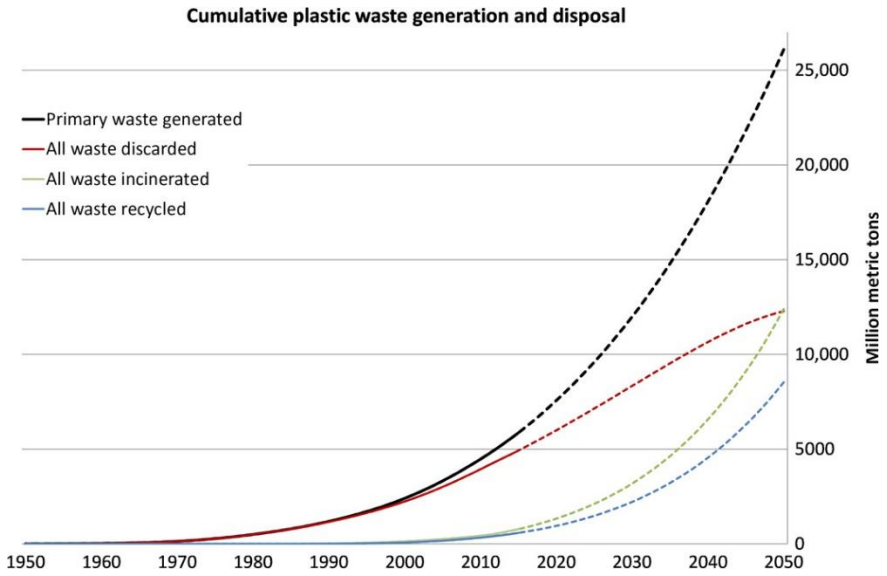

Figure 1. 1 *The exponential trajectory of plastic waste generation and disposal (in million metric tons), where solid lines represent historical data from 1950 to 2015, and dashed lines indicate the projections of the trends to the year 2050. [Source: Geyer et. al. 2017]*[8]

Atmospheric agents such as ultraviolet radiation, photodegradation, and biodegradation cause fragmentation of plastics into micro sized particles less than 5 mm in diameter, commonly known as microplastics (MP). MPs readily leach out of filtration systems and contaminate the human food chain, primarily through seafood consumption.[11,12] In fact, recent studies have found MPs in human placenta and bloodstreams.[13,14] The scale of damage and long-term toxicity to humans is not clear, but pose

genotoxic, carcinogenic and developmental toxicity.[15] These findings have shed light on the extent of human exposure to plastics due to poor waste management control.

Table 1. 1 *Plastic demand distribution by resin type in Europe 2019, and their applications.[4] PUR = Polyurethane. "Others" include acrylonitrile butadiene styrene (ABS), poly (butylene terephthalate) (PBT), and poly (methyl methacrylate) (PMMA).*

Polymer	Plastic Demand Distribution (%)	Applications
PP	19.4	Microwave containers, food wrappers, bank notes, automotive parts, facemasks.
LDPE/ LLDPE	17.4	Food packaging, films, carrier bags, trays
HDPE	12.4	Toys, milk bottles, shampoo bottles, houseware
PVC	10	Window frames, floor and wall covering, pipes, cable insulation
PET	7.9	Bottles for water, soft drinks, fizzy drinks, cleaning products
PUR	7.9	Pillows, mattresses, insulating foams
PS	6.2	Food packaging (dairy & fish), disposable cutlery and containers
Others	18.3	Optical fibres, touch screens, surgical devices and protective coatings

Plastics can be categorised into thermoplastics (pliable upon heating and solidifies upon cooling) and thermosets (irreversibly hardening polymers).[16] Thermoplastics are more often used in high-volume consumer goods, and the four most common type of consumer plastics are high and low-density polyethylene (HDPE and LDPE, respectively), polyethylene terephthalate (PET), and polypropylene (PP). These four plastics make up the largest share of municipal solid waste (MSW) streams in the packaging sector (40%).[4] HDPE and PET are commonly used for packaging in drink bottles, toiletries and cleaning products and have the highest recovery rates. Single use bags and films are composed of linear low-density polyethylene (LLDPE) and LDPE. Meanwhile, PP is used for packaging and containers such as bottles, caps, and tupperware (**Table 1. 1**).[4] Packaging products have shorter lifespans compared to other plastic markets such as building and construction and therefore dominate the MSW streams.[17] In the UK, 40.3% of kerbside waste collection was primarily comprised of PET,

followed by HDPE (21.6%), LDPE (~16%), PP (10.2%) and approximately 2% polyvinyl chloride (PVC) and polystyrene (PS).[18,19] Meanwhile, PP has the largest production demand in Europe (19.4%), followed by LDPE (17.45%), HDPE (12.4%), and PVC (10%) (**Table 1. 1**).[4] Plastic use can only be reduced to a certain extent, but production of virgin material can be reduced by recycling and utilising post-consumer recyclate (PCR) waste. HDPE is more readily recycled than LDPE, and roughly 1.75 kg of petroleum is required to make 1 kg of HDPE.[20] LDPE requires higher pressures and energy to manufacture, thus HDPE is commonly preferred over LDPE for its lower costs.[20] For these reasons, the focus of this project is on HDPE as it is more cost effective in regards to most plastic resins paired with high industrial demand.

1.2 The Plastic Market

From 2021 to 2028, the worldwide plastic market is predicted to rise at a compound annual growth rate of 3.4 % from USD 579.7 billion.[21] China currently holds the largest share of the market with over 31% of the world's plastic production.[4]

Furthermore, the ongoing COVID-19 pandemic is fuelling the demand for plastic in the medical industry.[22] To fulfil increasing demands, companies are expanding their production and supply capacities. For example, in 2020 ExxonMobil announced to increase their monthly production of PP by 1,000 tonnes to meet the demands for medical masks and gowns due to the spread of coronavirus.[23] Due to risks of virus contamination, personal protective equipment (PPE) cannot be reused, although efforts have been made to down-cycle face masks for infrastructure applications such as pavements.[24] As such, with high records of PPE production, the medical and institutional waste streams have suffered from severe disruption.[25] Over 3.4 million single-use face masks and shields have been discarded daily globally, alongside latex gloves, aprons and other PPE with many ending up in oceans and landfill.[26] The Ellen MacArthur Foundation estimates that by 2050 there will be more plastic in the oceans than fish. However, with the recycling challenges bought on by COVID-19, this may be sooner than expected.[27,28]

The plastic industry gives jobs to over 1.56 million people in Europe, with over 55,000 companies involving a majority of small and medium sized enterprises. A turnover of more than €350 billion was achieved in 2019 with a positive trade balance of €13.1 billion.[4] As a result, eliminating plastic would cause a major disruption in the economy and welfare of most, if not all countries. Therefore, alternative routes to material sustainability need to be considered, such as plastics recycling. When recycled correctly, plastics have the lowest carbon emissions compared to alternative packaging

materials such as aluminium or glass.[29] Banning or substituting other products for plastic can have serious adverse effects, such as increased greenhouse gas (GHG) emissions, water consumption, and food waste. Fortunately, plastic recycling rates have increased by more than 92% since 2006, owing to growing social awareness and introduction of government legislations such as the Circular Economy Package (CEP).[30,4]

It is challenging to recycle plastic effectively, and even if this is achieved once it only becomes more difficult for subsequent recycling cycles. This is due to thermo-oxidative degradation during mechanical recycling, which lowers the quality of recyclate. Therefore, new approaches and innovations are imperative if we are to close the loop and transition from a linear to a circular plastic economy.

1.3 The Circular Economy

The growth of plastic production and its lasting environmental damage is putting socioeconomic strain on industries to transition from a linear plastic economy to a closed loop system. In a linear plastic economy, raw materials are used to make a product, which is then used by consumers and discarded. On the other hand, in a circular economy, the lifetime of plastic is extended by recycling the plastic in a continuous loop, thereby minimising the amount of waste generated (**Figure 1. 2**). Therefore, resources will remain in use for as long as feasible whilst extracting the maximum value from them. As a result, a circular plastic economy will decrease the volume of production of virgin plastics whilst allowing demand to be met through post-consumer recycled plastics.

The CEP is focused on recycling 65 % of municipal plastic waste by 2035, as well as decreasing waste transported to landfills or incineration, allowing no more than 10 % municipal waste to go to landfill.[31] As such, the CEP makes it feasible to keep more recyclable items in circulation within the resource and waste systems, rather than incinerating or burying them.[32] In order to facilitate a circular economy, further legislations have been passed to introduce and enforce producer responsibility and specify recycling targets. The EU is seeking an 'improved' separate collection system by 2030, with 90% of single-use plastic bottles to be collected by 2025.[33] Germany, for instance, recycled 93.5% of its PET bottles in 2015, while Norway gathered 97% of its PET bottles, and France aspires to recycle 100% of plastic waste by 2025.[34,35,36] However, it is important to note that not all gathered plastics are recycled. The success of these countries hinges on enforcement of Extended Producer Responsibility (EPR) schemes and tax implementations. Out of the 28 EU member states, currently 26 have an EPR scheme, meanwhile the UK is set to employ this in 2023.[37] The outcome of a given EPR scheme will mean producers are assigned considerable financial and/or physical responsibility for the handling or disposal of post-consumer items by introducing mandatory policy targets. Therefore, plastics can be

disposed of in a sustainable manner which will enable an effective waste collection and recycling system.

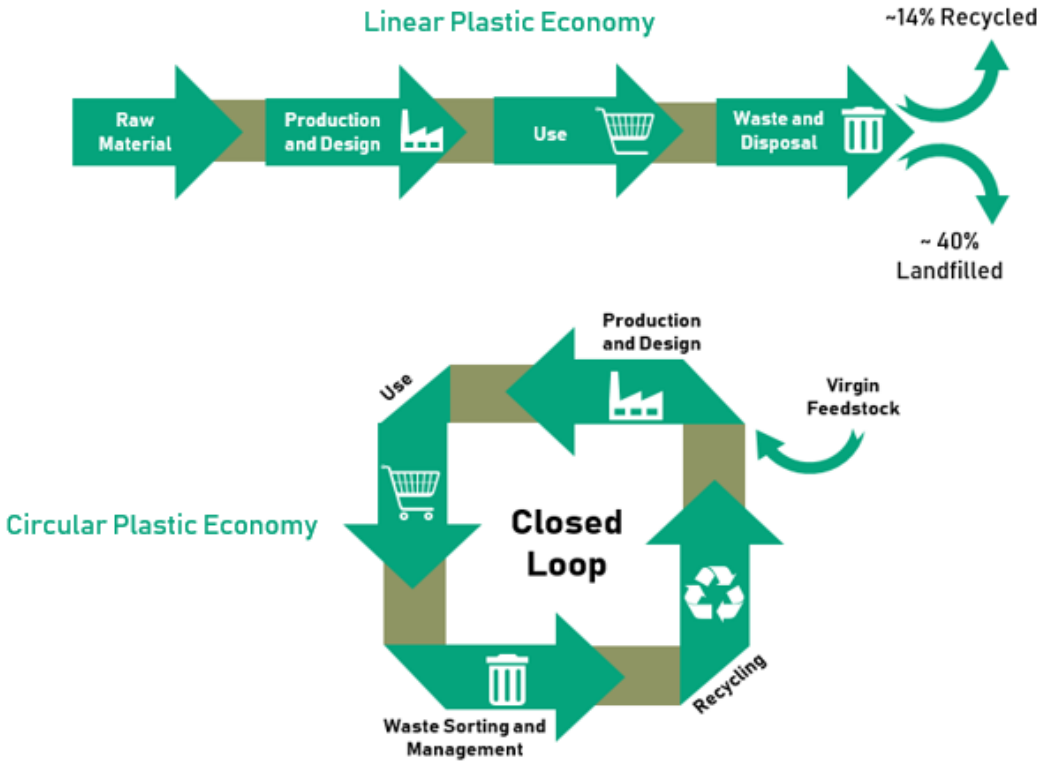

Figure 1. 2 *The linear plastic economy (top) and the circular plastic economy (bottom). The amount of virgin feedstock incorporated into recyclate in a circular plastic economy should preferably be zero. The values for landfilled and recycled content in a linear plastic economy were obtained from the Ellen McArthur Foundation.*

1.4 Plastic Advantages

There is a large misconception about the environmental effects of plastic production. The environmental effects of plastic waste are more of a concern than plastic production itself. In fact, only about 4% of the world's fossil fuel resources are used for manufacturing plastic.[38] Therefore, it is important to understand why recycling plastic is the priority rather than replacing it. Nearly two-thirds of GHGs arising from production and disposal of plastics are generated in the early production stages from the extraction of fossil fuels to resin production. Meanwhile, conversion of resins to bags, bottles, and other products emits just under one-third of emissions, with the remainder coming from waste disposal and management (**Figure 1. 3**).[29] This demonstrates that approximately 1,100 Mt of CO_2 emissions can be avoided if recycled resins were to be used opposed to virgin material.

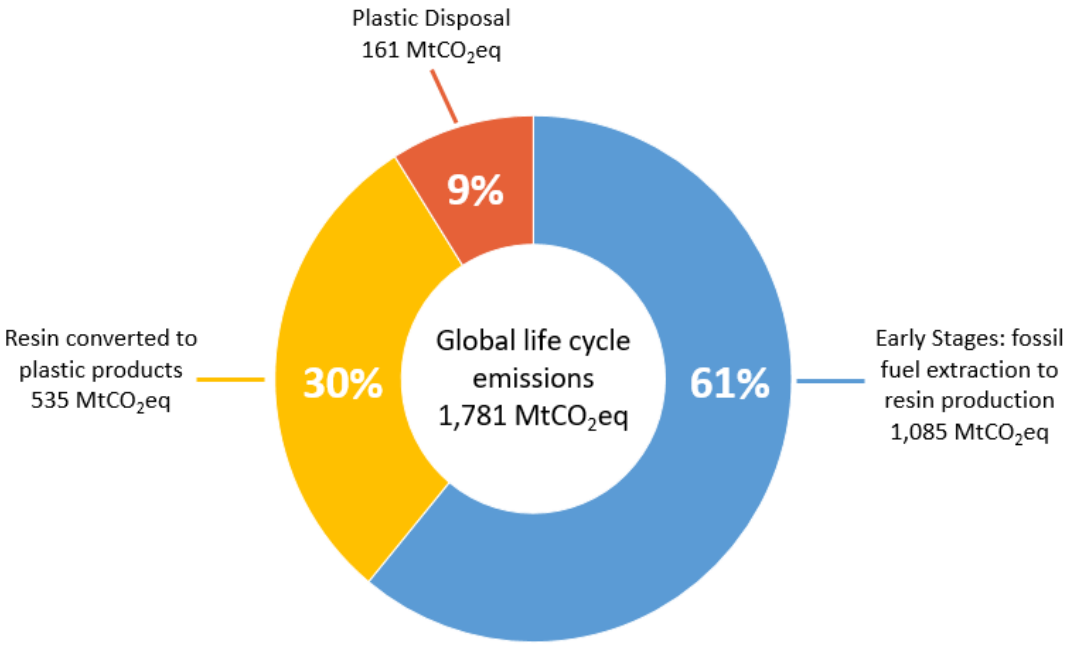

Figure 1. 3 *Lifecycle assessment of fossil fuel-based plastics measured in metric tons of CO_2 equivalent ($MtCO_2eq$), 2015.The global lifecycle emissions of plastics are 1,781 $MtCO_2eq$ with majority of emissions arising from the early production stages of fossil fuel extraction [Source: Voulvoulis et al. 2020].*[29]

Plastics are durable and lightweight, consuming significantly less fuel for transport and saving weight in automobiles, aeroplanes and packaging.[39] Replacing plastic packaging with alternatives such as aluminium, glass or cardboard would result in an increased weight per item, leading to higher energy and fuel consumption, alongside greater raw material costs and CO_2 emissions (**Figure 1. 4**).[29] Furthermore, the exceptional moisture and oxygen barrier properties of plastic limit produce degradation and therefore food waste. The European Commission adopted the European Strategy for Plastics in a Circular Economy in January 2018.[40] The strategy includes initiatives targeted at studying and understanding the life-cycle implications of using alternative feedstock for plastic manufacturing. A Life-Cycle Assessment (LCA) is used to determine how a product or process affects the environment. LCAs allow for the estimation of a products potential negative and positive consequences, some of which would be otherwise undetectable.

An LCA conducted by Amienyo et al. analysed the Global Warming Potential (GWP) of various drink packaging. It was found that of those analysed, glass possessed the highest GWP (555 g of CO_2 eq.) compared to PET which had the lowest (151 g of CO_2 eq.). [30] Additionally, if PET recycling rates were increased to 60%, a glass bottle would have to be reused 20 times to obtain the same reduced carbon footprint. Aluminium cans were also better than glass (312 g of CO_2 eq.), but still fared worse than PET. This was further supported by a study that reported that the carbon footprint for a virgin PET bottle was lower than a glass bottle with 80% recycled content, demonstrating that plastics are

superior to glass with regards to production and waste treatment methods.[41] Although plastics have a similar GWP to fibreboard packaging, plastics remain the more versatile and practical packaging option of the two. As such, it is significant to understand the importance of plastics and recycling, and why societally encouraged alternative materials are not preferable.

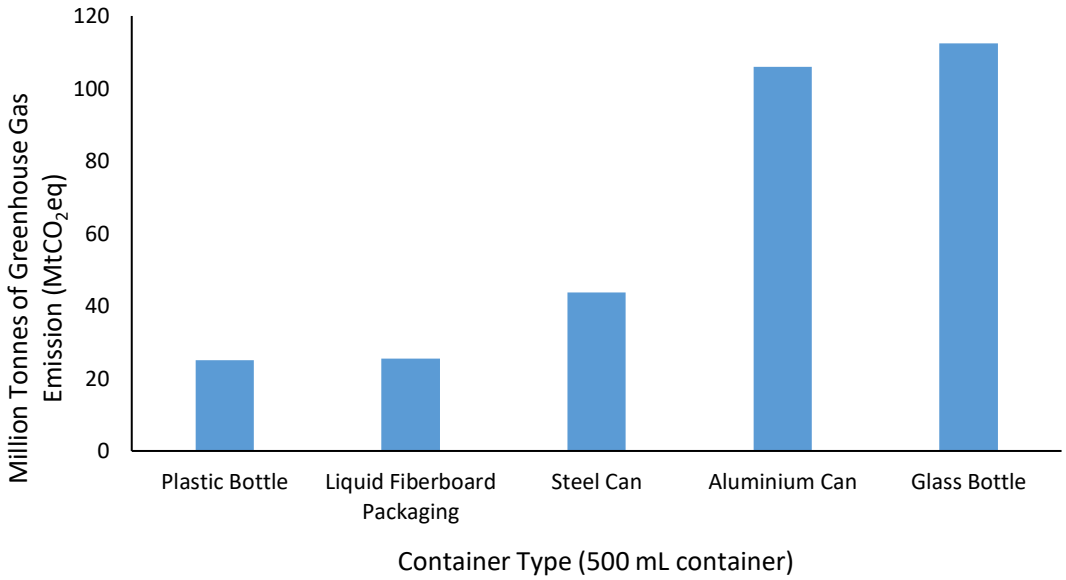

Figure 1. 4 *GHG emissions from 500 mL drink containers produced using plastic and alternative materials measured in million tons of CO_2 equivalent ($MtCO_2eq$), 2016. Out of the containers shown, glass bottles have the largest carbon footprint, meanwhile plastic bottles have the lowest [Source: Voulvoulis et al. 2020].*[29]

1.5 Polyolefins

Polyethylene (PE) is a type of thermoplastic formed by the free radical polymerisation of ethylene (**Scheme 1. 1**), where *n* represents the degree of polymerisation. Common initiators are organic peroxides which can generate free radicals to polymerise ethylene through a chain reaction mechanism.[42]

Different types of PE have the same basic repeating unit ($-CH_2-CH_2-$), but have different structural properties and applications. The density of PE has a direct correlation to the amount of branching along the polymer backbone. High molecular packing orders of the PE chains increases the density of the polymer matrix. This results in a more crystalline and opaque material. PE is relatively chemically inert as the types of reaction that PE is vulnerable to is limited by the small dipole moments between the C-C and C-H covalent bonds.[43]

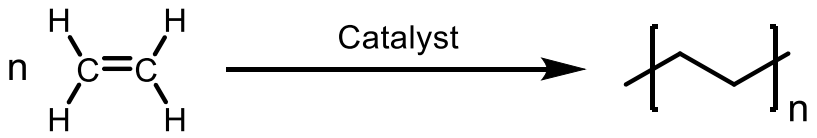

Scheme 1. 1 *Reaction scheme representing the polymerisation of ethylene, with the use of catalysts such as Ziegler-Natta, metallocene or Phillips, where n is equivalent to the number of monomers i.e. degree of polymerisation.*

The two main types of PE are LDPE (low-density) and HDPE (high-density). LDPE has low density due to long chain branching on the polymer backbone, which is a result of inter- and intramolecular charge transfers during polymerisation. This extensive branching hinders crystallisation, and therefore LDPE has a lower % crystallinity (i.e. is more amorphous) than HDPE. The lower crystallinity of LDPE gives rise to its valuable properties such as transparency and flexibility. On the other hand, HDPE is linear with very low levels of branching defects. The chains can pack more densely and therefore HDPE has a greater crystallinity and density than LDPE. As a result, HDPE is more rigid, opaque and has a higher tensile strength.[4] The rate of UV/biodegradation in the environment is dependent on the amorphous phase of the polymer, as such, for crystalline HDPE degradation is slower than LDPE as reduced chain mobility promotes radical recombination opposed to radical propagation reactions.[10,44] HDPE has a fair oxygen barrier and good moisture barrier, and a melting temperature (T_m) of around 135 ^oC which makes it suitable for high temperature applications.[45] The synthesis route for HDPE includes low pressures using either Phillips, Ziegler-Natta, or metallocene catalysts to control polymer topology.[46] The influence of such catalysts on polymer properties are summarised below:

<u>Ziegler-Natta</u>

The Ziegler-Natta (ZN) catalyst is a complex formed by the reaction of a transition metal compound with a metal alkyl or alkyl halide. The primary components of these catalysts are a support (e.g. $MgCl_2$), an active transition metal (e.g. $TiCl_4$) and a co-catalyst (e.g. triethylaluminium, $AlEt_3$).[47] Due to the heterogeneous nature of ZN catalysts with different active sites, the polymer properties can only be influenced to a certain degree.[48] One of the key characteristics of ZN catalysts are that they yield polymers with broad molecular weight distributions (MWD) i.e. large dispersity (Đ).[49,50] The competition between propagation and termination processes influences the length of the polyolefin chain.[51] Therefore, hydrogen gas can be fed into the reactor at specified pressures or amounts to control chain development. The resulting chain length(s) and dispersity will in turn affect the flow behaviour and processability of the polymer during recycling.

Metallocene

A typical metallocene catalytic system consists of a metallocene catalyst and co-catalyst (e.g. methylaluminoxane, MAO) (**Figure 1. 5**). A metallocene catalyst involves a π-bonded metal atom situated between aromatic ligands, typically involving cyclopentadienyl, indenyl and fluorenyl groups.[52] The variation of aromatic ligands, bridges, and metals gives a number of factors to tailor the polymerisation process and resulting polymer properties.[53] Unlike ZN systems, metallocene catalytic processes are homogenous. These catalysts are also known as single-site catalysts—each catalyst particle has only one active site—and they provide high reactivity and narrow MWD. As a result, metallocenes can be up to 100 times more active than ZN or Phillips catalysts.[52]

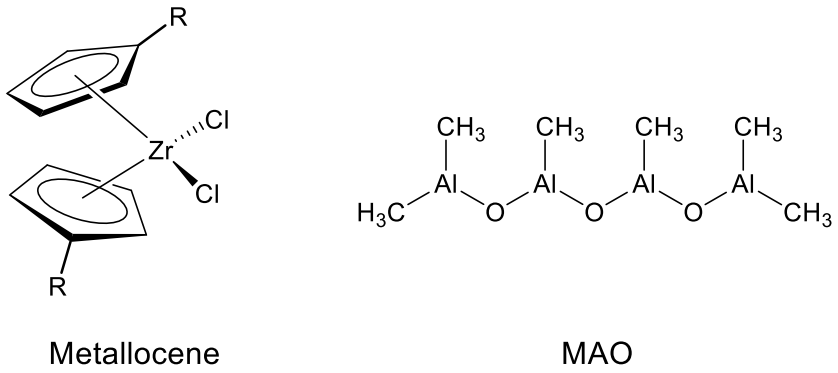

Figure 1. 5 *A simplified schematic representation of a metallocene catalytic system, consisting of a zirconium metallocene catalyst (left) and a methylaluminoxane co-catalyst (right).*[48]

Phillips Catalyst

The Phillips catalyst is a chromium-based catalyst on a silica support, and is used for almost half of the global HDPE production.[54] The Phillips catalyst provides the broadest molecular weight distribution of all three catalyst systems highlighted here. It also yields polymers with more shear-thinning behaviour with respect to the other two, meaning the molten HDPE flows more readily under applied stress. This is because the smaller MW chains act as a plasticizer between the larger MW chains, allowing chains to slide more readily with less chain entanglement and therefore improving the processability of the material during recycling. In general, ZN and Phillips catalysts yield linear polyolefins with no long-chain branching and a dispersity greater than 3.[55]

The two most important characteristics of HDPE are the MWD and degree of branching. High MW chains provide excellent mechanical strength, and the inclusion of low MW chain – in other words a

biomodal MWD adds the benefit of easy processability (**Figure 1. 6**).[56] The different types of catalysts affect the amount of long-chain branching, and in turn provide different flow characteristics (i.e. melt flow index) to the polymer resins.

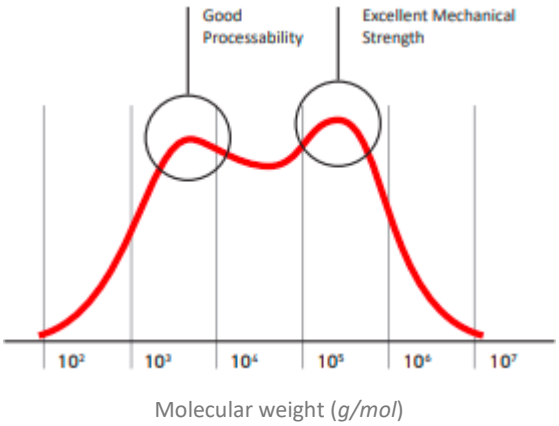

Figure 1. 6 *A bimodal type molecular weight distribution, where the low MW fractions provide good processing properties, and the high MW fractions improve mechanical strength [Source: MolGroupChemicals].*[56]

With decreased branching, the melting point, density, stiffness, tensile strength, crystallinity, and modulus of elasticity increases, thus providing a range of attributes for the manufacturer.[57] For this reason, there is no competition in the market between HDPE grades derived from different catalysts, but rather each serves a unique purpose in the market's demands. Therefore, the recycling properties of HDPE grades will vary when processed.

1.6 Recycling of Polyolefins

The 4 main types of polymer recycling methods are: primary (mechanical closed-loop recycling), secondary (mechanical recycling into lower value products), tertiary (depolymerisation) and quaternary recycling (energy recovery).[58] Primary recycling, also known as closed-loop recycling consists of extruding pre-consumer or pure post-consumer materials into products of similar value.[19] Whereas secondary recycling involves the extrusion of plastic waste into lower value products. On the other hand, tertiary recycling is the chemical depolymerisation of polymeric waste into its monomeric feedstock. And finally, quaternary recycling is the pyrolysis of plastics for energy recovery, commonly used on materials which are not suitable for recycling through the former three methods. However, this approach is least favourable due to the release of GHG's during pyrolysis.[19]

1.6.1 Mechanical Recycling

1.6.1.1 Sorting of Plastic Waste

The first steps in the value chain of mechanical recycling is collection, sorting and cleaning of plastic waste. There are significant limitations to plastic recycling bought on by contaminated waste streams. The mixing of different waste streams leads to poor final performance of recyclate due to different working temperature and intrinsic incompatibility between polymers. The free energy of mixing (ΔG_m) two polymers is governed by the Flory-Huggins interaction parameter, χ, in which miscibility can only be achieved when ΔG_m is negative.[59] The difference in molecular size and topology between polymers means there is ineffective stress and strain transfer between the phase boundaries, increasing the free energy of the system and lowering the mechanical properties of the polymer blend.[19] For a binary system, the Flory-Huggins parameter can be expressed using the following equation:

$$\Delta G_m = RT \left[\frac{\phi_1}{r_1} ln\, \phi_1 + \frac{\phi_2}{r_2} ln\, \phi_2 + \chi \phi_1 \phi_2\right] \quad \textbf{(1. 1)}$$

Where R is the universal gas constant, T is the absolute temperature, ϕ_i represents the volume fraction of the species and r_i is the number of polymer segments, which in this case is proportional to the degree of polymerisation. Polymer compatibility can be improved via surface modification and use of compatibilisers to reduce interfacial tension and increase intermolecular interactions.[60] However, this approach often makes the different components in the overall material difficult to separate. As a consequence, the material is not recyclable by conventional means such as extrusion. By contrast, bulk plastics—if effectively sorted to relatively pure waste streams—are suitable feedstock's for extrusion

1.6.1.2 Extrusion

Mechanical recycling through extrusion entails melting and homogenising of raw material using shear force and high temperature. Polymer is fed into the extruder via the hopper (**Figure 1. 7**), where it is melted (plasticized) and mixed using the shear-force of rotating screws. Up to four screws can be used in an extruder depending on the application.[61] Although single-screw extruders can be cheaper, twin-screw extrusion is preferable for polymer recycling as the recyclate is subject to less shear and allows uniform homogenisation. This reduces both shear and thermal degradation because of less residence time in the barrel.[62] The screws can either be co-rotating (rotation in the same direction) or counter-rotating (rotation in opposite directions). Some advantages of co-rotating screws is the self-wiping ability requiring less cleaning, alongside less screw and barrel wear.[63]

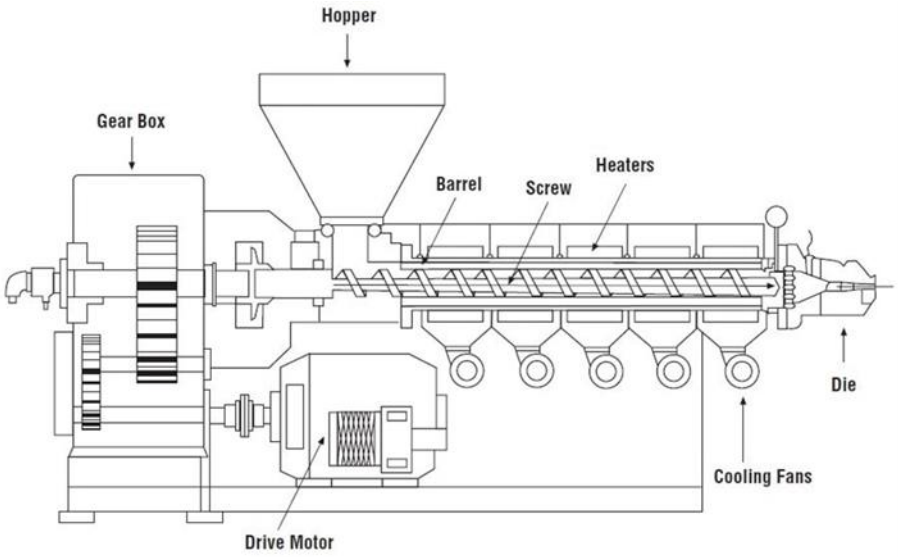

Figure 1. 7 *A simplified schematic diagram of a single screw extruder. [source:* Azo Materials*].*[64] *In this project a co-rotating twin-screw extruder was used.*

Once the molten stream of polymer exits the die, the extrudate needs to be cooled below T_m or T_g to ensure dimensional stability. It is commonly cooled in a water bath and solidified to the desired shape whilst being pulled away from the extruder at a constant velocity to maintain the desired cross-section. The extrudate can then be processed through injection moulding, film blowing, and other methods.[65,-66]

In a standard extrusion process, the specific mechanical energy (SME) measures the amount of mechanical energy (work) put into the extrudate as shown in the equation below.[67]

$$SME = \frac{2\pi \times n \times T}{MFI} \qquad \textbf{(1. 2)}$$

Where *T* is the torque (Nm), *n* is the extruder speed (RPM) and MFI is the melt flow index (g/10min). The mechanical energy put into the extruder is transformed into heat through viscous dissipation. SME is also dependent on the feed rate and temperature, both which influence the torque output of the extruder. SME increases with increasing viscosity, increasing screw speed and decreasing MFI. It is an important parameter in mechanical processing used the characterise the extrusion process, and governs the quality characteristics of the recyclate.[68] MFI is an important parameter to characterise virgin polymer and recyclate (discussed in more detail in section **1.6.1.3**), and has significant influence on the SME during extrusion. Low MFI grades will increase the SME due to having higher viscosities,

which requires greater screw speed and higher temperatures to increase flow rate. As such, low MFI HDPE grades require greater mechanical energy for processing during recycling.

1.6.1.3 HDPE Processing

HDPE is commonly processed between 160–230°C.[7,70,71] Lower temperatures have shown to cause less chain scission and degradation and are overall better for preserving polymer properties.[72] The processing conditions for HDPE are typically based on the properties of the material, namely its melt flow index (MFI). MFI is an industrially-relevant measure of the ease of flow of a thermoplastic polymer. It measures the rate of extrusion of thermoplastics at a specific load and temperature and is given in g/10 min.[73] MFI values are given in polymer specification and data sheets for quality control purposes, and are an indirect measure of MW, where high MFI values correspond to lower MW polymer.[74] The zero shear viscosity (η_0) is directly proportional to the polymer's molecular weight for low MW polymers as chain entanglement is not a factor.[75] However, above a critical MW, M_C, the dependence of the zero shear viscosity on MW becomes significantly more pronounced because the chains begin to entangle. For entangled polymer melts, mathematical models using power laws have been developed to predict the weight average molar mass (M_W). These models predict that $\eta_0 \propto M_W^3$ although the empirical relationship is closer to $\eta_0 \propto M_W^{3.4}$. For linear polymers, models have shown an inverse relationship between MFI and MW whereby $1/MFI = (M_W)^x$ (where x = 3.4–3.7).[76] Beyond the Newtonian region, the melt viscosity of HDPE decreases with increasing shear rate, which is known as shear thinning. Due to speeding up the material flow, minimising heat generation, energy consumption, and SME, this property is an essential non-Newtonian trait in polymer processing.

The rheological behaviour of HDPE can be expressed in terms of complex viscosity, η*, which measures the overall resistance to flow with respect to angular frequency (ω). The angular frequency measures the rate of oscillatory shear flow in rad/s during dynamic rheology measurements. Complex viscosity (η*) can be calculated using the complex modulus, G*, which is the total resistance against deformation of a material. The relationship between complex viscosity and modulus is shown in the equation below:

$$\eta^* = G^*/\omega \qquad \textbf{(1. 3)}$$

G* is comprised of elastic and viscous components which contributes to the materials overall stiffness. Through measuring G* as a function of angular frequency, the complex viscosity of HDPE can be obtained.[77] The Cox-Merz rule predicts that the magnitude of the complex viscosity, $|\eta^*(\omega)|$ is

proportional to the steady shear state viscosity, η(γ̇) when shear rate, γ̇ is equal to ω.[78] However, the significance of the Cox-Merz rule is strongly influenced by polymer structure, molecular weight and chain entanglement, thus will not hold between different grades of HDPE.[79]

Another key consideration for HDPE processing is the water content of the plastic. Even though polyethylene is not hygroscopic, polar contaminants within PE can allow moisture sorption which can negatively affect the properties of the bulk material. The higher the degree of crystallinity, the lower the water equilibrium content will be. This results from the lower diffusion coefficient of water in the crystalline phase. At high temperatures during extrusion, water can become steam, resulting in bubbles, structural stresses and deformation. With each extrusion cycle the recyclate becomes more prone to water absorption due to the changes in the polymer structure from oxidative degradation. Therefore, it is necessary to dehumidify the material ahead of time. This can be a time consuming process, and long drying hours can affect the material properties.[80] This problem can be circumvented by co-extruding PCR material with zeolites (4A and 13X) which showed effective desiccant functionality during processing.[81] In fact, once compatiblised with maleic anhydride, the mechanical properties of the co-extruded polymers were comparable to those prepared by standard drying in a vacuum oven. Additionally, the zeolites were able to absorb undesirable odours, which is a problem that is often faced when working with PCR waste.[82]

1.6.1.4 Thermo-Oxidative Degradation

Thermo-oxidative degradation is accompanied by the loss of useful mechanical properties and discolouration.[83] Processing conditions including temperature, screw speed, feed rate and residence time influence the degradation kinetics of HDPE.[84] Degradation predominantly takes place in the amorphous phase of polymers, and therefore the degradation kinetics between HDPE and LDPE will vary.[85] The deterioration of polymer properties increase with oxygen content under atmospheric conditions, and was demonstrated by Gijsman et al. where the elongation at break of PP films decrease with increasing oxygen uptake (**Figure 1. 8**). The thermo-mechanical stresses generated by the screws cause hydrogen abstraction along the polymer chain, yielding macro-radicals. Under low concentrations of oxygen, these macro-radicals predominantly react with each other to form branches and crosslinks, increasing MW. If oxygen is present in high concentrations, then the macro-radicals react with the oxygen resulting in radical propagation, in which unstable compounds attack the polymer backbone leading to chain scission (decreasing MW) and formation of carbonyl end groups.[86] Spectroscopic measurements such as Fourier Transform Infrared Spectroscopy (FT-IR) can be used to detect presence of carbonyl end groups by measuring carbonyl concentration i.e. carbonyl index (CI), indicating the amount of degradation.

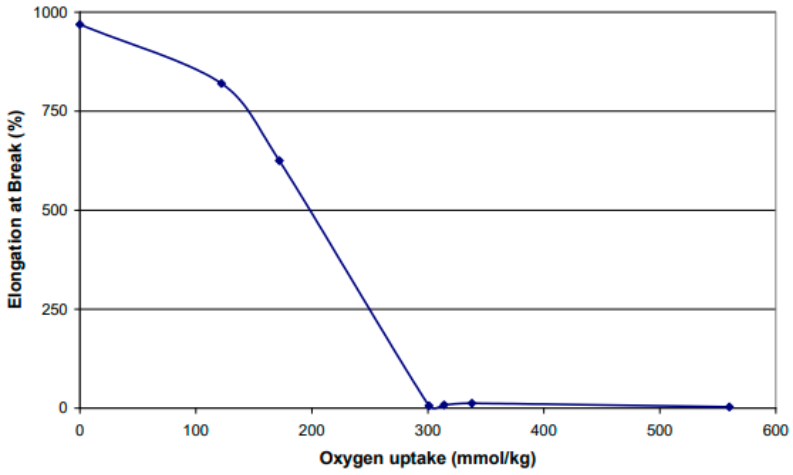

Figure 1. 8 *The relationship between elongation at break (%) and oxygen uptake (mmol/kg) of PP films. The elongation at break decreases with increasing oxygen uptake and plateau's around 300 mmol/kg [Source Gijsman et al. 1996].*[87]

Thermo-oxidative degradation includes initiation, propagation and termination steps as shown in **Scheme 1. 2**. During the initiation step, light absorbing groups, such as impurities from catalyst residues or chromophores, produce radicals under UV light. During the propagation step, oxygen will react with the alkyl radicals to give peroxy radicals (ROO·). The reaction rate of oxygen with alkyl radicals is fast, instantaneously leading to peroxy radicals.[88] The peroxy radicals can then abstract a hydrogen atom from the polymer chain to yield more alkyl radicals (R·) and hydroperoxides (ROOH). The hydroperoxides are decomposed into radicals which can abstract a hydrogen from the polymer chain and yield further alkyl radicals that will re-initiate the propagation step. The chain reaction will continue until a termination step is reached, in which two radicals can react to form a non-radical species. The rate determining step of the thermo-oxidative degradation mechanism is the abstraction of hydrogen requiring the breakage of a C-H bond.[89]

Oxygen enters the extruder in two ways, through adsorption on the surface of the polymer and dissolution in the amorphous phase.[90] As such, it may be possible to minimise thermo-oxidative degradation during mechanical recycling if extrusion was to be carried out in an inert atmosphere. Epacher et al. found that HDPE extruded under air had a higher MFI than samples extruded under argon atmosphere, with more discolouration (higher yellowness index) present under normal atmospheric conditions.[83] Discolouration can result from direct oxygen-stabilizer interactions, as well as secondary reactions involving alkyl and alkoxy radicals and antioxidants.[83]

Although thermo-oxidative degradation could be minimised by extrusion in inert atmosphere, degradation cannot completely be eliminated during recycling. Thermo-mechanical degradation induced by temperature and shear stress can still yield macro-radicals resulting in chain scission and branching of polymer chains even under low oxygen concentrations.

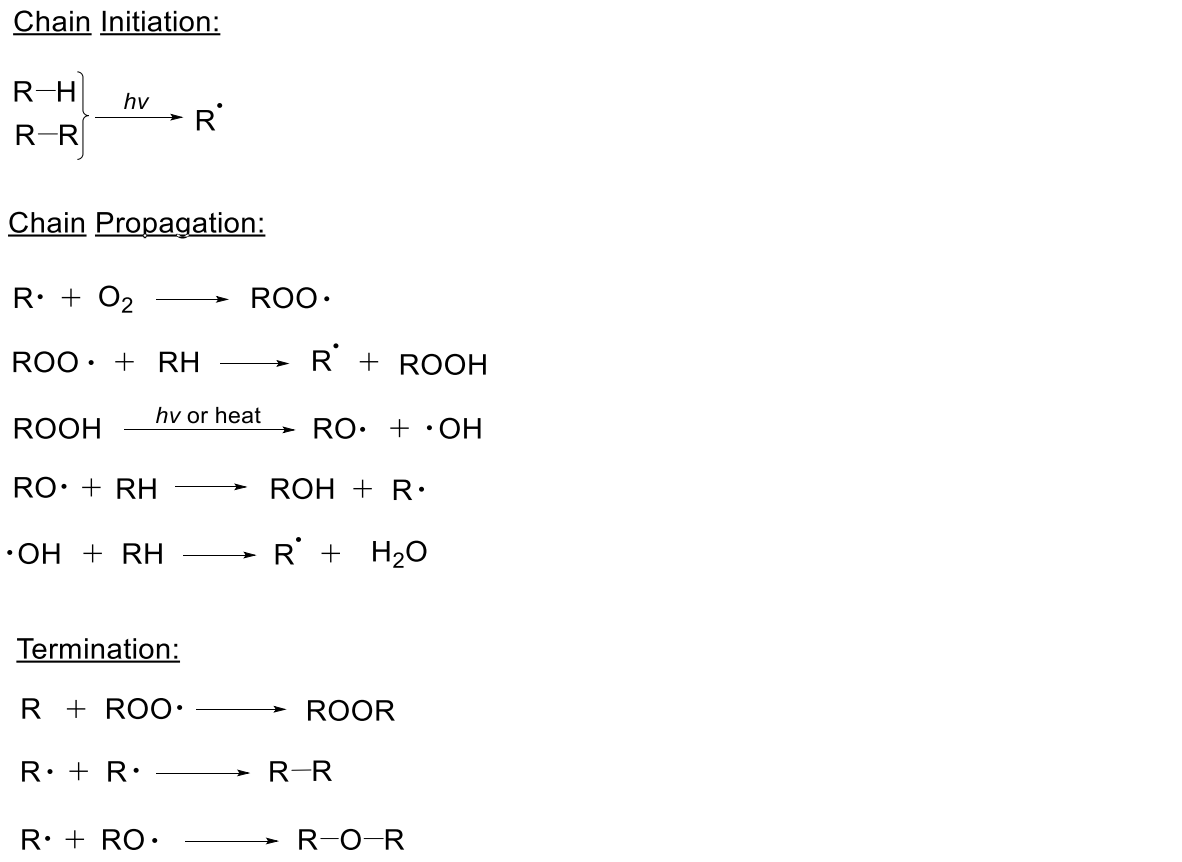

Scheme 1. 2 *General reaction scheme of thermo-oxidation of polymers including chain initiation, propagation and termination steps where R represents polymer backbone.* [89]

1.6.1.5 Chain Scission and Branching

It has been reported that the rate of chain scission is directly proportional to the chain length of the polymer.[91] Longer chains are more likely to undergo chain scission due to molecular entanglement, whereas shorter, mobile chains are more susceptible to branching and crosslinking.[92] Consequently, properties such as the rheology and flow of the polymer (e.g. MFI) is affected. Chain-scission commonly increases the MFI, and chain branching and cross-linking decrease MFI. With HDPE produced using a Phillips catalyst, cross-linking is dominant during recycling, whereas with a Ziegler-Natta catalyst chain scission is prominent.[93] The effect of reprocessing on the MFI of HDPE is not clear. Some authors report that MFI increases with the number of reprocessing cycles,[70,94] others notice

decreases,[92,95,96] and some report no significant changes at all.[91,97] As a result of these inconsistencies, it was concluded that variations in MFI must be related to the choice of catalyst during polymerisation and additive content.[98] The change in properties of HDPE resulting from chain scission and branching mechanisms will affect the processability of the material during recycling. A decrease in MFI will make the recyclate difficult to process and extrude, whereas an increase in MFI will improve processability but will likely lower mechanical properties.

In a study of 100 consecutive extrusion cycles on HDPE, the viscosity of molten HDPE was found to oscillate between cycles; this result was an indication of simultaneous chain scission and branching.[98] The MWD was found to broaden over sequential cycles, which can be explained as follows: the chain branching and cross-linking generates higher MW chains, whereas lower MW chains are formed through chain scission.[98] Thus, it is commonly accepted that HDPE undergoes chain branching and scission simultaneously during reprocessing.[92,91,99] However, not much is known as to how different HDPE grades, additive formulations and catalysts, affect this mechanism, or whether process control can be achieved. Control of reaction mechanism (i.e. relative extents of branching/crosslinking vs. chain scission) by selection of additives and catalysts could enable fully tailored recycling of the material, and enable a predictive understanding of recycling HDPE with various grades and properties

1.6.2 Additives

Plastic materials are formulated with different additives to improve performance, functionality and ageing.[100] The most commonly used additives are plasticizers, flame retardants, antioxidants, anti-static and slipping agents, acid scavengers, UV/heat stabilizers and pigments.[101] Each additive has a distinct functionality for enhancing the final properties of plastic, and are divided into four main categories[102]:

- **Functional additives** (flame retardants, stabilisers, plasticizers, anti-static and slip agents, curing agents)
- **Colorants** (pigments and fluorophores)
- **Fillers** (clay, calcium carbonate, mica, and even coffee grounds)[103]
- **Reinforcements** (glass fibres and carbon fibres)

Additives are usually not chemically bound to the polymer. Only reactive organic additives such as flame retardants can occasionally be polymerised into the polymer chain.[100] To achieve circularity, plastics need to be recycled efficiently into materials with good performance; advances in polymer additive technology could therefore be a significant factor in making this a reality. BASF has recently announced a novel additive formulation (IrgaCyle) which can enhance the quality of PCR polyolefins

by enhancing stability and processability of the recyclate.[104] However, companies such as BASF do not disclose which additives are in their formulations due to intellectual property and patent restrictions.

One of the most pervasive categories of additives in polymer production and recycling are antioxidants. Polymers can readily undergo reactions with oxygen during production and use. The mechanical properties of the material are reduced due to free radical reactions and discolouration is often observed.[105] The most common method of inhibiting thermal oxidation is the use of stabilizers i.e. antioxidants (AO), which are typically only needed in small amounts (up to 2% w/w). Hydrogen abstraction from the polymer—the rate-determining step in PE degradation—is inhibited because the AOs contain a more readily extractable hydrogen.[89] Examples of common industrial antioxidant tradenames are Irganox 1010, Irganox 1076 and Irgafos-168 (**Figure 1. 9**).[89] There are two classes of antioxidants, each described in more detail below:

Primary Antioxidants

Primary AOs are also known as free-radical scavengers. The most common primary AOs are sterically hindered phenols and aromatic amines. Phenolic oxidation can occur in the presence of ZN or metallocene catalyst residues.[106] The main mechanism with phenolic AOs involves a hydrogen abstraction from the phenolic O–H group (or N–H group in aromatic amines) to form a phenoxy radical. This radical is stable due to both steric hindrance and resonance, and therefore, at ambient temperatures it does not abstract a hydrogen atom from the polymer backbone and inhibits radical initiation. Although phenolic AO are generally resistant to discolouration, when oxidised, they form quinones with conjugated double bonds. These chromophores can absorb light and result in yellowing of polymer resins.[107] This is unfavourable during polymer processing and reduces the value of the recyclate. However, high MW phenolic AOs with large bulky substituents can sterically hinder such oxidation reactions and result in less yellowing.[106] Epacher et al. processed HDPE with different concentration of stabilizer (Irganox 1010) up to 7 extrusion cycles.[96] With increasing stabilizer concentration, the discolouration—quantified via a defined yellowness index (YI)—increased linearly. However, even in the absence of any stabilizer, slight discolouration was still present meaning that colour change cannot solely be due to stabilizers, and that there are likely other impurities present (or formed during extrusion) that cause discolouration.

There are also naturally occurring phenols, such as α-δ tocopherols (Vitamin E), curcumin, β-carotenes and ascorbic acid with antioxidant properties and have been utilised as stabilizers for plastics.[108,109] For example, Olejar et al. extracted grape tannin from agro-waste wine for its antioxidant properties,

and significant improvement in anti-oxidant activity was seen at 1% incorporation of tannin in polyolefin films including HDPE.[110]

Secondary antioxidants

Secondary AOs are also known as hydroperoxide decomposers (HD). These react with hydroperoxides (ROOH) by abstracting an oxygen atom to yield more stable alcohol (ROH) species. Secondary AOs are often used with primary AOs because they work in concert with one another to provide more protection to polymers, usually preserving the melt flow properties and colour stability more effectively during repeated processing cycles. They are considered cost effective when they can reduce the required amount of more costly primary AOs.[107] Of the various options for secondary AOs, phosphorus compounds are widely preferred due to their low toxicity. Phosphorus compounds are oxidised into phosphates when they accept an oxygen atom from hydroperoxides, leaving behind stable non-radical species.[111] However, they are susceptible to hydrolysis reactions which forms acids and affects the polymer MFI. It can also result in corrosion and breakdown of additives into smaller molecules which can migrate through the polymer matrix, an unfavourable consequence for food packaging and water pipe applications.[107]

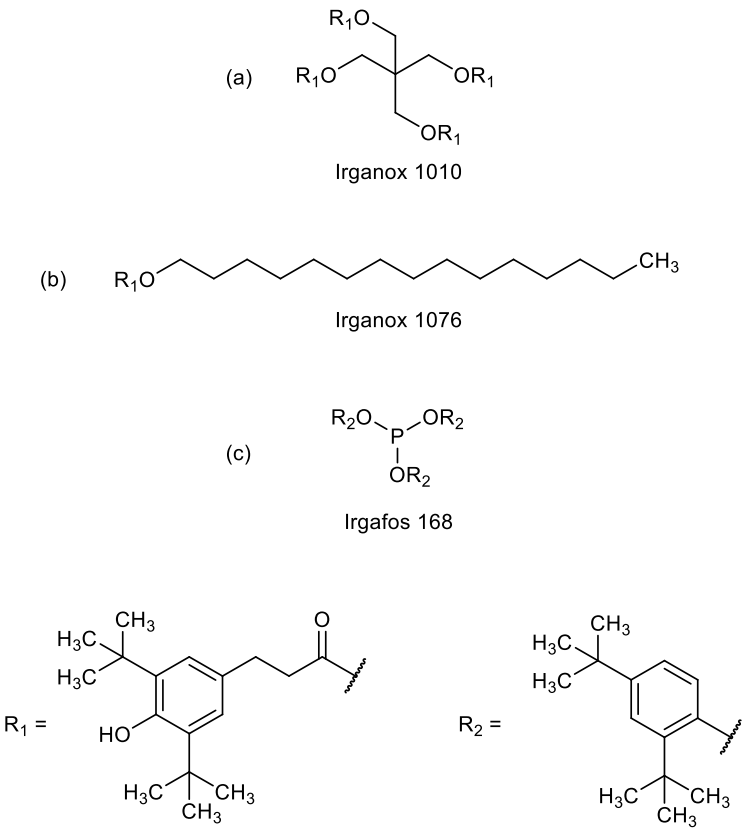

Figure 1. 9 *Simplified chemical structures of common antioxidant additives including (a) Irganox 1010 (b) Irganox 1076 and (c) Irgafos 168 where R groups represent the phenolic groups.*

Another important additive category for HDPE are UV stabilisers. These protect against photo-oxidative degradation, which is an outcome of the combined mechanism of UV radiation and oxygen, deteriorating the mechanical and physio-chemical properties of polymers. The most important classes of UV stabilizers are Hindered Amine Light Stabilizers (HALS), benzophenones/benzotriazoles, and organic nickel compounds.[112] Titanium dioxide can also be used, but is expensive and some side effects such as cell damage and genotoxic effects can arise.[113] Protection from light has also been achieved through the use of carbon black.[114] However, carbon black results in contamination and sorting complications during recycling as it disrupts the signal of optical recognition instruments such as FT-IR spectroscopy. In addition to UV stabilizers, plasticizers are also commonly used to reduce chain entanglement.

Overall, the incorporation of distinct formulation of stabilizers changes the behaviour of polymers during production and recycling. Understanding the design and mechanism behind additive formulations within polymer grades, and its implications on recycling can help tailor plastic materials to function within a circular economy.

1.7 Project Objectives

This project focuses on the mechanical processing of HDPE. Recycling was simulated by performing multiple extrusions and analysing subsequent changes to the properties of the plastic. Although extrusion is the most common recycling method, variations of recycling-induced property degradation has not been investigated between different chemical grades of the same material. For example, HDPE can be polymerised using different catalysts and can possess varying amounts of UV and thermal stabilisers, which in turn can affect its degradation behaviour.[115,116] Furthermore, differences in molecular weights between HDPE grades can result in variations in melt flow index and viscosity due to chain entanglement and molecular mobility. This in turn determines how the material will behave when subject to extrusion conditions and recycling. It is hypothesised that low MFI grades will likely better retain their mechanical properties, but may result in more discolouration during repetitive recycling. This assumption is based upon the fact that greater MW polymers (i.e. low MFI) have a greater degree of chain entanglement and therefore more stress resistance. However, low MFI grades require more mechanical energy and higher temperatures during processing, which may result in more thermo-mechanical/oxidative degradation and discolouration.

The main objectives of this project were to: 1) explore the properties of various virgin HDPE grades from different manufacturers, 2) carry out 5 extrusion cycles on HDPE grades from one manufacturer (ExxonMobil) to simulate mechanical recycling, 3) characterise the recyclate quality of recycled HDPE

grades through various analytical techniques. The techniques include rheology, tensile testing, differential scanning calorimetry (DSC), UV-Vis colorimetric analysis and Fourier-transform infrared (FTIR) spectroscopy. Understanding the relationship between properties of HDPE grades and their degradation kinetics during recycling will aid the selection and development of recyclable HDPE, facilitating the optimisation of materials to maximise recycling cycles. This work will therefore contribute to the effort of keeping more plastic in closed-loop circulation, thus reducing the reliance on virgin feedstock.

2 Materials and Methods

2.1 Materials

Methanol (CH_3OH, 99.8 %) and Toluene (C_7H_8, 99.7 %) were supplied from Sigma Aldrich, Chloroform ($CHCl_3$, 99 %) from Acros Organics and Hexane (C_6H_{14}, 99 %) from Fisher Scientific. All HDPE grades were provided by Hardie Polymers. HMA014, HMA016 and HMA018 were manufactured by ExxonMobil™. HI7052B was manufactured by CIPLAS™, and HD85612 by SIBUR™. The specifications including density and melt flow index (MFI) are shown in **Table 2.1** below.

Table 2. 1 *Specifications of different HDPE grades including density, MFI, melting temperature and stabiliser content. No stabiliser information was given for grade 4. No peak melting temperature was given for grade 5, besides the Vicat Softening Temperature which is 127 °C.*

Grade	Density (g/cm^3)	MFI (g/10min)	Thermal Stabiliser	UV Stabiliser	Peak Melting Temperature (°C)
1 HMA014 (Exxon)	0.960	4	Yes	Yes	134
2 HMA016 (Exxon)	0.956	20	Yes	No	133
3 HMA018 (Exxon	0.954	30	Yes	No	131
4 HI7052B (Ciplas)	0.952	6.8	-	-	131
5 HD85612 (Sibur)	0.961	8.5	-	Yes	-

2.2 Sample Preparation

2.2.1 Extrusion

Mechanical recycling was simulated by extrusion cycles. Prior to this, the polymers were dried in Fistreem Vacuum Oven equipped with an Edwards RV5 vacuum pump (70 °C for 4h or 58 °C for 16h) to avoid hydrolysis and chain scission due to the presence of excess water. Extrusion cycles were performed on a Thermo Scientific™ HAAKE Process 11 co-rotating parallel Twin-Screw Extruder with a screw diameter of 11mm, and length of 40 L/D. 1.5 kg of HDPE pellets were processed at various temperatures depending on their MFI and properties (**Table 2. 2**). The extrudates were then passed through a water bath (20 °C) to cool the material before pelletising, and then pelletised using a Thermo Scientific™ HAAKE Varicut Pelletizer to yield pellets of 1.5 mm in size. The feed rate was increased from 2% from the first cycle up to 30% due to reduction in pellet size. After each cycle roughly 100 g of sample was retained for analysis.

Table 2. 2 *Extrusion temperatures and rotation speeds used in the extruder barrel during mechanical recycling of HDPE grades HMA014, HMA016 and HMA018.*

Grade	Barrel Temperature (°C)								Rotation Speed (RPM)
	Zone 2	Zone 3	Zone 4	Zone 5	Zone 6	Zone 7	Zone 8	Die	
1. HMA014	180	180	200	200	200	220	220	230	300
2. HMA016	150	180	180	180	180	200	200	200	200
3. HMA018	150	180	180	180	180	180	180	180	200

2.2.2 Injection Moulding

The dumbbell-shaped specimens were made using a HAAKE Minijet II at a pressure of 400 bar. The mould and cylinder temperatures were 80 °C and 200 °C respectively, and the dwelling time was set to 5 seconds. The mould dimensions were specified according to the ISO 527-2-1BA standard (**Figure 2. 1**). Although ISO states that the length of the 1BA specimens is 55 ± 2 mm, the length was found to be 50 mm when measured using callipers. The product data sheet states that the dimensions of the mould vary slightly to BSI standards.

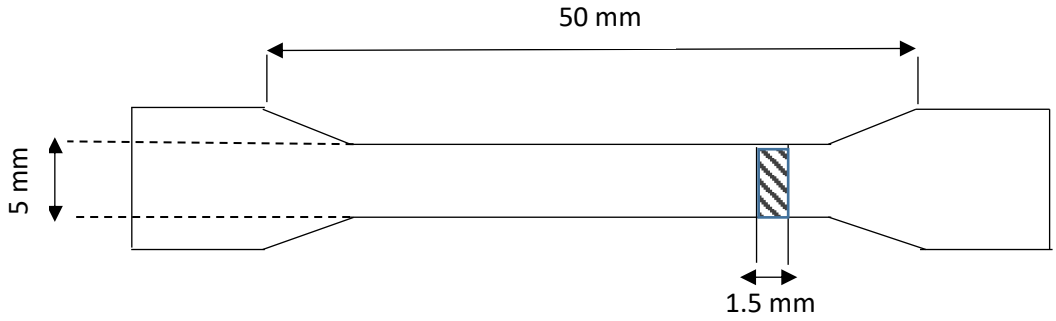

Figure 2. 1 *Schematic illustration of the dimensions for dumbbell shaped specimens used in tensile testing, with a length, width and thickness of 50 mm, 5 mm and 1.5 mm, respectively.* (Not to scale).

2.3 Rheology

Rheological measurements were conducted on HDPE pellets using a Discovery Hybrid Rheometer-2 (TA instruments) and a steel Environmental Test Chamber (ETC) equipped with 25 mm parallel plate geometries. Frequency sweeps were performed at the average HDPE processing temperature of 180°C to simulate the rheological behaviour during mechanical recycling. The angular frequency was varied from 0.1 to 500 rad/s in a logarithmic manner, at a 1 % strain collecting 5 points per decade. All samples were trimmed at 1050 mm, then lowered to the measuring gap at 1000 mm before running measurements.

2.4 Differential Scanning Calorimetry

All DSC measurements were conducted on TA Instruments DSC 2500. The measurements were taken on samples of 3–7 mg obtained from HDPE pellets which were cut in half using pliers. The samples were placed in T_{zero} pans fitted with $T_{hermetic}$ lids, and an equilibration step was run at -80 °C. The samples were then heated from -80 to 300 °C at a scan rate of 10 °C·min^{-1} to erase the thermal history, and then cooled back down to -80 °C at a scan rate of 10 °C·min^{-1}. No cold crystallisation peaks were present in the thermal scans. The percentage crystallinity was calculated according to the relationship shown in equation (**2. 1**) below, where ΔH_m is the measured melting enthalpy and ΔH_0 has a value of 293 J/g for 100 % crystalline PE.[117]

$$\%\ \boldsymbol{Crystallinity} = \left(\frac{\boldsymbol{\Delta H_m}}{\boldsymbol{\Delta H_0}}\right) \boldsymbol{X\ 100} \qquad \textbf{(2. 1)}$$

2.5 Fourier-Transform Infrared Spectroscopy

FTIR measurements were performed using a Bruker Invenio-s on polymer pellets which were flattened using pliers. Soxhlet extracted samples were measured in solution by dissolving the extracts in 15 ml of solvent (chloroform or hexane). Background scans were taken of the solvents prior to any measurements. For both solid and liquid state measurements, 64 scans were performed with a resolution of 4 cm^{-1} from 4000-400 cm^{-1} using transmission mode, and the absorbance spectra was analysed using the Bruker software.

2.6 Mechanical Testing

Tensile tests of dumbbell-shaped HDPE specimens were carried out on an Instron Universal Testing Machine (series 3344) using a 500 N load cell at a crosshead speed of 50 mm/min as stated in ISO 527-2/1A/50. Five specimens for each recycling cycle were tested, each having a length, width and thickness of 50 mm, 5 mm and 1.5 mm respectively.

The Young's Modulus (*E*), Yield Strength (σ_m) and Strain at Break (ε_b) were then measured. *E* was calculated from the slope of the stress/strain curve in the strain interval between 0.05 % and 0.25 % according to ISO-527-1:2012 standards.[6]

2.7 Colour Measurements

A UV-Vis spectrophotometer (PerkinElmer, Lambda 365) was used to calculate the Yellowness Index (YI) and colour change of HDPE with respect to extrusion cycles. The measurements were conducted on 1.5 mm thick dumbbells (see **Section 2.2.2**) at room temperature and pressure.

L*, a* and b* values were obtained using a CIELAB colour space model (**Figure 2. 2**) to measure colour change, *ΔE*, as shown in equation (**2. 2**) below.

$$\Delta E^*_{ab} = \sqrt{(\Delta L^*)^2 + (\Delta a^*)^2 + (\Delta b^*)^2} \quad \textbf{(2. 2)}$$

A small *ΔE* value implies that there is minimal colour change. The L* value gives the lightness of an object i.e. a white object has an L* value of 100 and a black object has 0. Whereas the chromatic colours are represented by a* (+ red, - green) and b* (+ yellow, - blue).

YI is the degree to which an object's hue shifts from colourless or a favoured white to yellow, and was calculated according to the ASTM E313-20 standard using the equation below.

$$\boldsymbol{YI} = \frac{\boldsymbol{100(C_x X - C_z Z)}}{\boldsymbol{Y}} \quad \textbf{(2. 3)}$$

Where X, Y and Z are the measured tristimulus values of the material calculated for illuminant D65, while C_x and C_z are coefficients obtained from the ASTM standard.

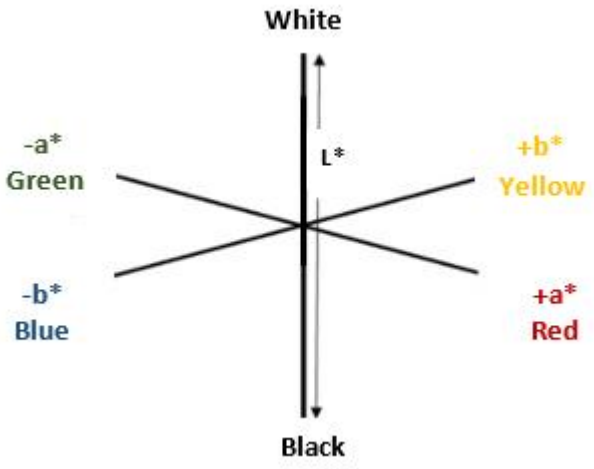

Figure 2. 2 *Representation of the CIEL*a*b colour space model. Where 'a' represents green to red, and 'b' represents the yellow to blue axis. L* depicts the perceptual lightness. [Adapted from Viscarra et. al. 2006]*

2.8 Soxhlet Extraction

Soxhlet extractions were carried out on the HDPE grades to extract additives. Chloroform (250 mL) was measured into a 500 mL round bottom flask. HDPE pellets (20 g) were weighed into a cellulose extraction thimble (Whatman 60) and placed into the soxhlet extractor (**Figure 2. 3**). The mixture was then refluxed for 24 h at 110 °C and 250 RPM. A waterless condenser was used (Asynt, Condensyn 450 mm), and once the extraction time had elapsed, the solution was allowed to cool to room temperature before concentrating to dryness in a rotary evaporator. The resulting product resembled a white/pink stain mark on the bottom of the round bottom flask. This was then washed 3 times with chloroform (15 mL) in order to remove the sample from the round bottom flask, then transferred to a 30 mL vial. PE has poor solubility in methanol (MeOH), therefore in order to remove any low molecular weight oligomers, a small portion of the chloroform sample (5 mL) was pipetted into an auto sampler vial and kept for separate analysis, whilst the rest (10 mL) was mixed with MeOH (20 mL). After shaking the mixture, a white precipitate (PE) formed which were then removed by filtering through cellulose filter papers (Whatman 1).

Meanwhile, the steps for soxhlet extraction was repeated on the same HDPE pellets using hexane (250 mL). Hexane is less polar then chloroform and was therefore predicted to extract the non-polar fractions. The same steps for washing and filtering were also repeated using hexane as the solvent,

then both chloroform and hexane extracts were evaporated on a hotplate at 40 °C and kept for further analysis.

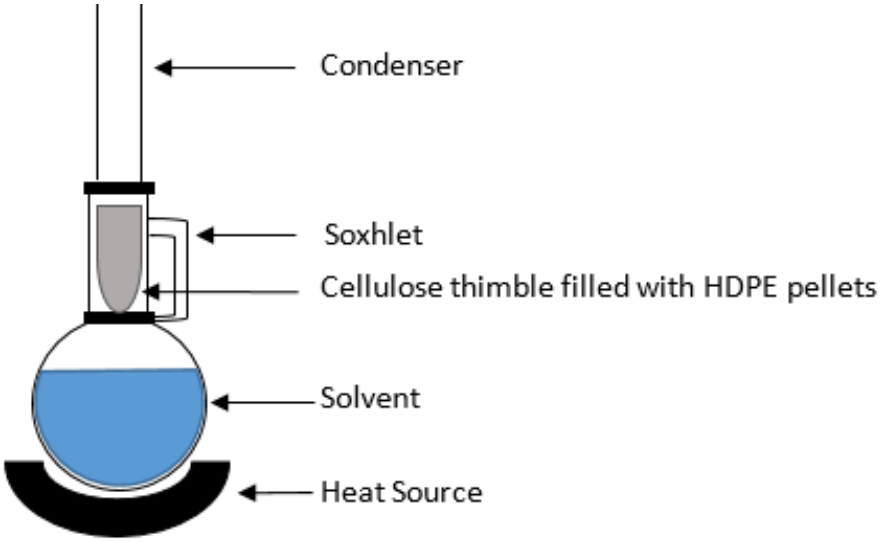

Figure 2. 3 *A simplified schematic diagram of the soxhlet extraction apparatus, which was performed at 250 RPM and 110 °C.*

2.9 Cryogenic Milling

HDPE pellets (4 g) were first dried in a vacuum oven (Fistreem equipped with an Edwards RV5 vacuum pump) at 60 °C for 4 hours. The pellets were then placed in a 50 mL stainless steel jar with a 20 mL ball bearing and placed into a cryomill (Retsch 207490001). The instrument was pre-cooled using liquid nitrogen to -196 °C for 7.5 minutes at 5 Hz prior to the grinding cycles. Three milling cycles were performed at 25 Hz for 3 minutes with intermediate cooling times of 1.5 minutes at 5 Hz. Once finished, the resulting HDPE powder was dried in a vacuum oven overnight at 45 °C.

2.10 Error Calculations

Standard errors were obtained through calculating the standard deviation, σ, and dividing by the square root of the sample size as shown in the equations below:

$$\sigma = \sqrt{\frac{\sum(x_i - \mu)}{N}} \qquad \textbf{(2. 4)}$$

Where N is the sample size, x_i is each value from the sample, and μ is the sample mean. The standard error, SE, was then calculated using equation (**2. 5**)

$$SE = \frac{\sigma}{\sqrt{N}} \quad \textbf{(2. 5)}$$

3 Results and Discussions

3.1 Analysis of Virgin HDPE Grades

3.1.1 Mechanical, Thermal, and Rheological Properties

Virgin HDPE grades were analysed to understand the relationships between their properties and MFI. The samples include three grades from ExxonMobil™ (HMA014, HMA016 and HMA018) and further two grades from CIPLAS™ and SIBUR™. The mechanical, thermal and rheological properties are summarised in **Table 3. 1.**

Table 3. 1 *Properties of different HDPE grades. MFI and density were obtained from the technical data sheet provided by the polymer manufacturer. % crystallinity was calculated using the enthalpy changes acquired through DSC, and viscosity measurements were gathered through frequency sweeps at 180 °C. Tensile strength was obtained through tensile testing on injection moulded dumbbells at a rate of 50 mm/min.*

Grade	MFI g/10min	Density g/cm³	Crystallinity %	Viscosity at 0.1 rad/s (Pa.s)	Viscosity at 25 rad/s (Pa.s)	Shear Thinning Index	Tensile Strength (MPa)
HMA014	4.0	0.960	71.9	2594	559	13.2	27.6
CIPLAS™	6.8	0.952	67.7	1688	749	2.39	23.5
SIBUR™	8.5	0.961	73.7	1438	819	1.83	27.8
HMA016	20	0.956	64.5	523	412	1.55	24.3
HMA018	30	0.954	61.6	389	316	1.42	22.4

All grades display shear thinning properties, where viscosity is decreasing with increasing frequency (**Figure 3. 1**). The shear thinning intensity (i.e. shear thinning index) was calculated using the ratio of viscosities between 0.1 and 100 rad/s. These values were used because the variation in non-Newtonian behaviour between grades were more pronounced in that region. The data revealed that

shear thinning behaviour increases with decreasing MFI (**Table 3. 1**). This could be because high MW chains exhibit more chain entanglement. It is hypothesised that under shear force the magnitude of disentanglement and alignment along the direction of shear is more pronounced than lower MW chains.

Grades with higher MFI show lower viscosities at the zero-shear viscosity region (**Figure 3. 2**). This is the region in which a constant viscosity is observed at very low shear-rates, and the material is essentially at rest. At zero-shear viscosity (η^0), the MW of the polymer is proportional to its viscosity, however, once a certain level of MW is exceeded above the critical entanglement, the viscosity is proportional to the 3.4th power of the MW (**Equation 3. 1**) as discussed in the previous sections (**Section 1.6.1.3**).[119]

$$\eta^0 \propto M^{3.4} \; when \; (M \geq M_c) \qquad \textbf{(3. 1)}$$

Where M_c is the critical entanglement MW. When the MW exceeds M_c there is a significant increase in viscosity which supports the presence and influence of chain entanglement on the physical properties of the material.[119]

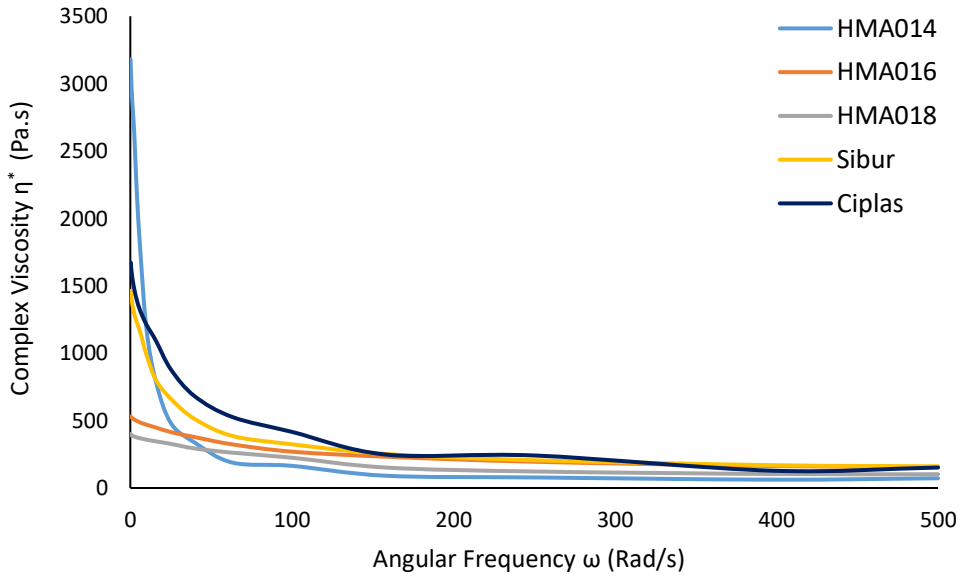

Figure 3. 1 *Decrease in complex viscosity (Pa.s) with increasing angular frequency (Rad/s) of HDPE grades including HMA014, HMA016, HMA018, Sibur and Ciplas. Viscosity measurements were obtained through frequency sweeps on HDPE pellets at 180 °C.*

The strong correlation (R^2 = 0.82) in **Figure 3. 2** confirms the expected relationship between MFI and viscosity.[120] An R^2 value below 0.5 is a poor correlation, above 0.5 is moderate, and values above 0.7 show a substantial fit.[121] Smaller MFI values (longer chains) experience more chain entanglement which causes resistance to flow, thus, increase viscosity. However, at higher shear rates, this trend is

disrupted (**Appendix 7.1.2**). The variation of polymer properties under different shear rates could be a result of the shear dependent motion of polymer chains under entanglement.

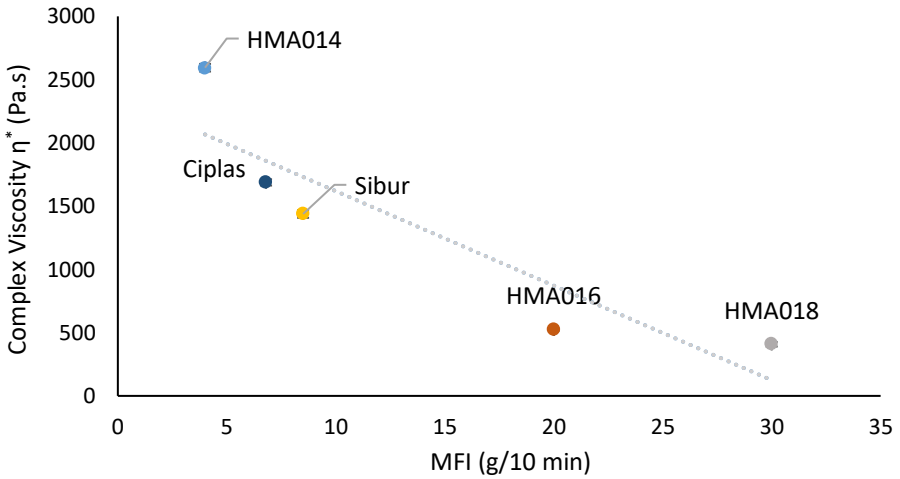

Figure 3. 2 *Increase in MFI (g/10min) with decreasing complex viscosity (Pa.s) of HDPE grades at 0.1 rad/s (R^2 = 0.82). The MFI was obtained through the polymer specification sheets provided by the manufactures, and viscosity was measured on HDPE pellets through frequency sweeps at 180 °C. Standard errors were calculated over three tests.*

Figure 3. 3 shows the relationship between the MFI and crystallinity of the HDPE grades tested. The crystallinity increases with decreasing MFI. High crystallinity reduces the mobility of the adjacent amorphous phases and therefore reduces polymer flow.[122] The crystalline domains have less free volume (higher packing density) and thus a more crystalline polymer has a higher density (**Figure 3. 4**). The reaction conditions may have been controlled to tailor HDPE chains with a narrow molecular weight distribution and low dispersity index. Additionally, the use of different catalysts and amount of co-monomer used during polymerisation is proportional to the number of side chains.[56] As a result, increased branching will decrease the crystallinity and density of polymers.

Figure 3. 5 to **Figure 3. 7** show further correlations between grade-based properties. As seen previously, Ciplas and Sibur typically do not fit the trend. This is likely because they are supplied by different manufacturers, whereas HMA014, HMA016 and HMA018 are manufactured by ExxonMobil, thus, are likely to use the same catalysts. The complexity of HDPE grades and variations can arise from the synthesis process, catalysts, blending of different MWs, chain branching and additive formulations.[123] Although ExxonMobil has a number of patents for metallocene catalysts, no specific catalyst information could be found for HDPE, thus, conclusions cannot be made on the polymerisation parameters.[124,125] However, if metallocene was used for these grades, then a narrow MWD would be expected.

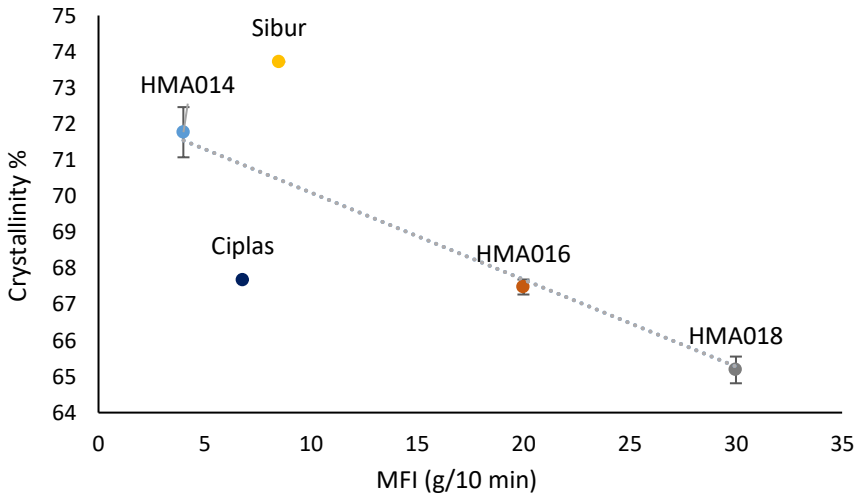

Figure 3. 3 *Decrease in % crystallinity with increasing MFI of HDPE grades (R^2 = 0.57). MFI was obtained through the polymer specification sheets provided by the manufacturers, and crystallinity was calculated from the enthalpy changes acquired through DSC. Standard errors were calculated over three tests.*

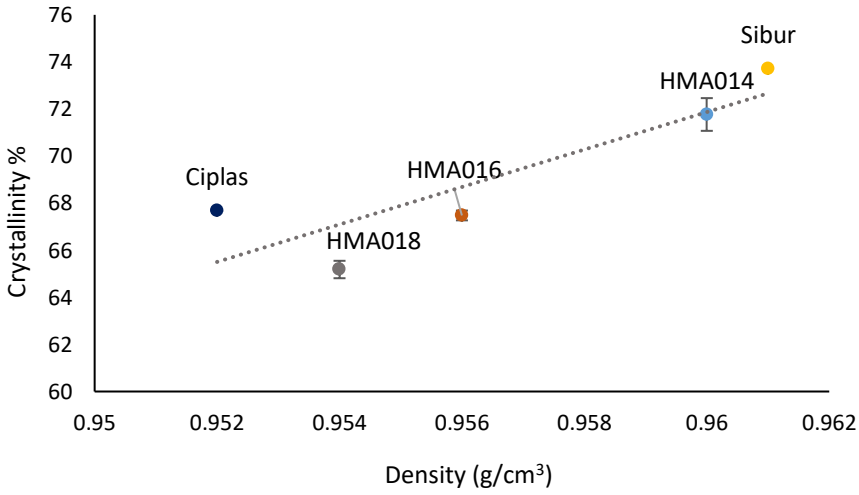

Figure 3. 4 *The increase in density with respect to crystallinity of HDPE grades (R^2 = 0.77). The density was obtained through the specification sheet of the polymer grades supplied by the manufacturers, and crystallinity was calculated from the enthalpy changes acquired through DSC measurements. Standard errors for % crystallinity were calculated over three tests.*

At high average MW the mechanical properties would likely be enhanced but have low processability. However, at a lower average MW the mechanical properties would likely be poorer but have better processability. Future work should entail size-exclusion chromatography (SEC) to obtain the MWD to predict the likely catalysts that may have been utilised during polymerisation.

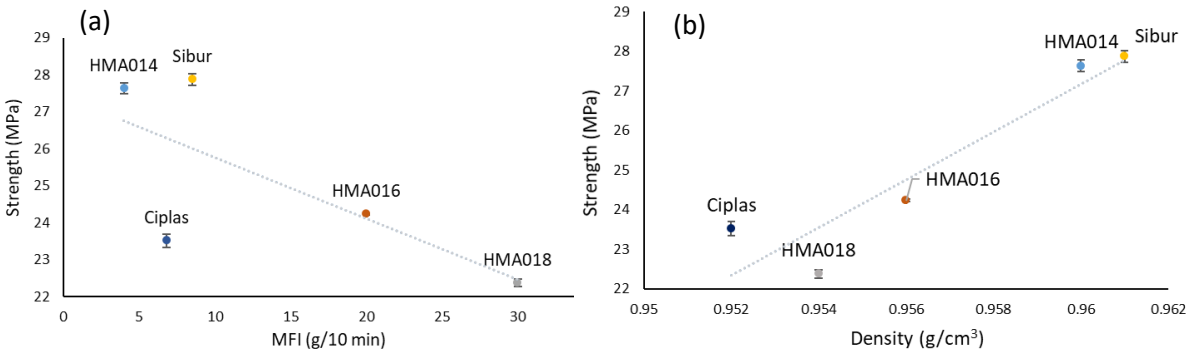

Figure 3. 5 *Relationship between tensile strength, MFI and density. Where (a) strength decreases with increasing MFI, R^2 = 0.52 and (b) strength increases with increasing density, R^2 = 0.87. Tensile tests were performed on injection moulded dumbbells at a rate of 50 mm/min. The density was obtained from the polymer specification sheets provided by the manufacturers. Standard errors for tensile strength was calculated over five tests.*

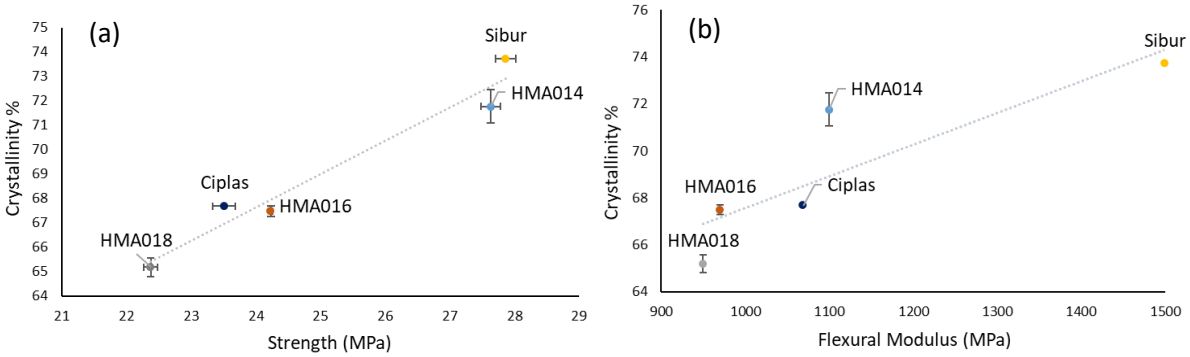

Figure 3. 6 *Relationship between crystallinity, tensile strength (MPa) and flexural modulus (MPa). Where increasing % crystallinity increases the (a) tensile strength, R^2 = 0.96 and (b) flexural modulus, R^2 = 0.75. The tensile strength was obtained through tensile testing on injection moulded dumbbells at a rate of 50 mm/min. The flexural moduli was obtained through the polymer specification sheets provided by manufacturers. Standard errors for % crystallinity were calculated over three tests, whereas for tensile strength the standard error was calculated over five tests.*

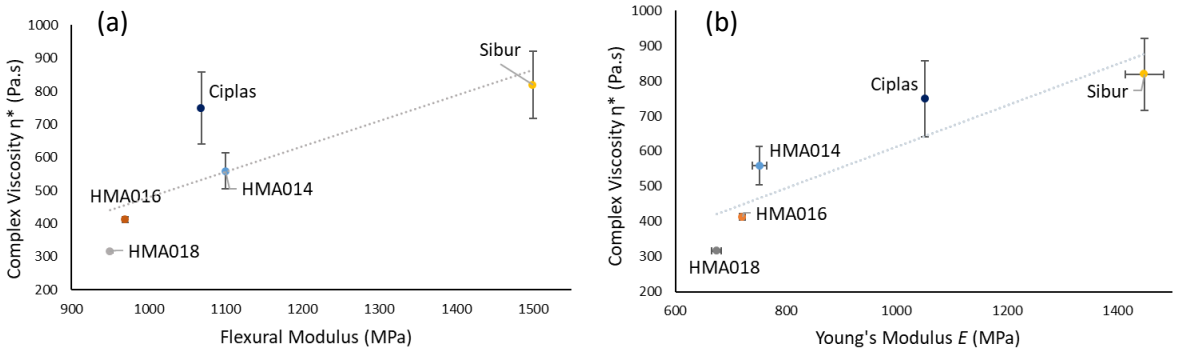

.

Figure 3. 7 *Relationship between complex viscosity (η*) measured at 25 rad/s and (a) flexural modulus and (b) Young's modulus (E). Where (a) flexural moduli increases with viscosity, R^2 = 0.64 and (b) Young's moduli increases with viscosity, R^2 = 0.81. Viscosity measurements were obtained through frequency sweeps conducted on HDPE pellets at 180 °C. Young's modulus was measured by tensile testing on injection moulded dumbbells at a rate of 50 mm/min, and flexural moduli were acquired through the polymer specification sheets provided by the manufacturers. Standard errors for η* were calculated over three tests, whereas for E, the standard errors were calculated over five tests.*

Excluding Ciplas, the tensile strength increases with decreasing MFI and increasing density (**Figure 3. 5**). This is expected because higher MW chains are typically stronger owing to chain entanglement, resulting in a stiffer material with greater creep resistance. However, high density materials tend to be less ductile and more susceptible to stress cracking due to restricted chain mobility. As seen previously, density and crystallinity have a direct relationship, therefore it is expected that higher crystalline grades show stronger mechanical properties (**Figure 3. 6**). High % crystallinity reduces the molecular free volume for chain entanglements in the amorphous phase and increases brittleness.
The degree of crystallinity governs the magnitude of secondary inter-intra chain bonding, which in turn influences the strength of thermoplastics. In fact, the degree of crystallinity has more influence over the mechanical properties of HDPE than the MW.[126]

Although Ciplas does not fit the trend, the viscosity of HDPE grades also increases with crystallinity (**Appendix 7.1.2**). Viscosity is measured above the melt temperature of the polymer, T_m, therefore HDPE is amorphous and not semi-crystalline in the molten state. However, a correlation is still seen between the molten and solid state of HDPE. The proposed explanation for this is that grades with more % crystallinity have a higher fraction of high MW chains, and increases the viscosity of the material in the molten state due to chain entanglement. As such, this also reflects on to the mechanical properties (**Figure 3. 7**). Flexural and Young's modulus increase with viscosity due to the similar effects of high MW chains in the molten and solid state, and has been shown that chain entanglement in the melt is largely preserved upon solidifying.[127]
The relationship between properties in the melt and solid phase are seen due to mutual interpenetration of MW and entanglement effects on different properties. Although this is expected, this data effectively highlights these correlations and shows that properties in the melt phase also transcend into the solid phase due to the MW relationship.

Overall, these results partially support the hypotheses and show that low MFI grades have greater mechanical properties, and whether the mechanical properties are retained after recycling is analysed in the next sections (**Section 3.3**). The correlations between the properties of HDPE grades would mean one property can be sufficient to estimate how the material will behave, saving experimental costs and energy for plastic manufacturers. These correlations are not novel, but by highlighting these relationships in a straightforward manner, as shown in the graphs above, it will be less time consuming and enable easier selection of HDPE grades for its intended use and recycling. This means that DSC, rheology and tensile testing will not be required at such extensive rates to predict material properties. For example, by only knowing the MFI, we can estimate the MW and viscosity of the material, and in turn the crystallinity and strength of the plastic through means of a multiple linear regression model.

However, complications arise when comparing grades from different manufacturers, therefore, this theory only applies to polymer grades from the same supplier as they are more likely to use the same catalysts and similar additives.

One of the main drawbacks is the lack of clarity on the synthesis of the chosen HDPE grades. Understanding the influence of catalytic polymerisation routes on mechanical, thermal, and rheological behaviour will aid the design of HDPE and better tailor its properties. Additionally, 5 variables are not enough to make a definitive conclusion regarding grade-based properties. More data and inclusion of a greater range of HDPE grades would give a solid foundation of information which could be correlated to map different characteristics.

3.1.2 FTIR Analysis

FTIR analysis was conducted to analyse structural differences between polymer grades. This would improve understanding between structure and property relationships.

Characteristic HDPE bands are located at 2916 cm^{-1} (asymmetric C-H stretch), 2848 cm^{-1} (symmetric C-H stretch), 1473 cm^{-1} (C=C vibration) and 730 cm^{-1} (C-H bend) (**Figure 3. 8**). Varying degrees of branching in polyethylene commonly results in small, but significant differences in the 1300-1400 cm^{-1} region and are due to methyl bending deformations of branched chain ends.[128] Minor discrepancies can be seen in the 1300-1400 cm^{-1} region for the ExxonMobil grades, which could be an indicator of chain branching. Additionally, the high MFI grades (HMA016 and HMA018) show similar patterns in the 1100 cm^{-1} and 800 cm^{-1} region. Short-chain ethyl branching has been previously identified around 770 cm^{-1} by other authors.[129] However, due to distorted baselines in the spectra, it is not possible to conclude the branching effects. The FTIR measurements were run on HDPE pellets which are too thick for transmission mode analysis which may be why the baseline is distorted. Reflective mode analysis on polymer pellets, or preferably transmission mode analysis on thin films (<50 μm) with increased number of scans are likely to improve the signal-to-noise ratio. [130]

Overall, the relationships between mechanical, thermal, and rheological properties of HDPE grades have been confirmed, and has been found that correlations are stronger in grades from the same manufacturers (i.e. ExxonMobil) opposed to different suppliers (Sibur and Ciplas). This is likely due to similar additives and polymerisation routes using the same catalyst. Further understanding of additive content will help understand the influence of stabilisers on polymer properties.

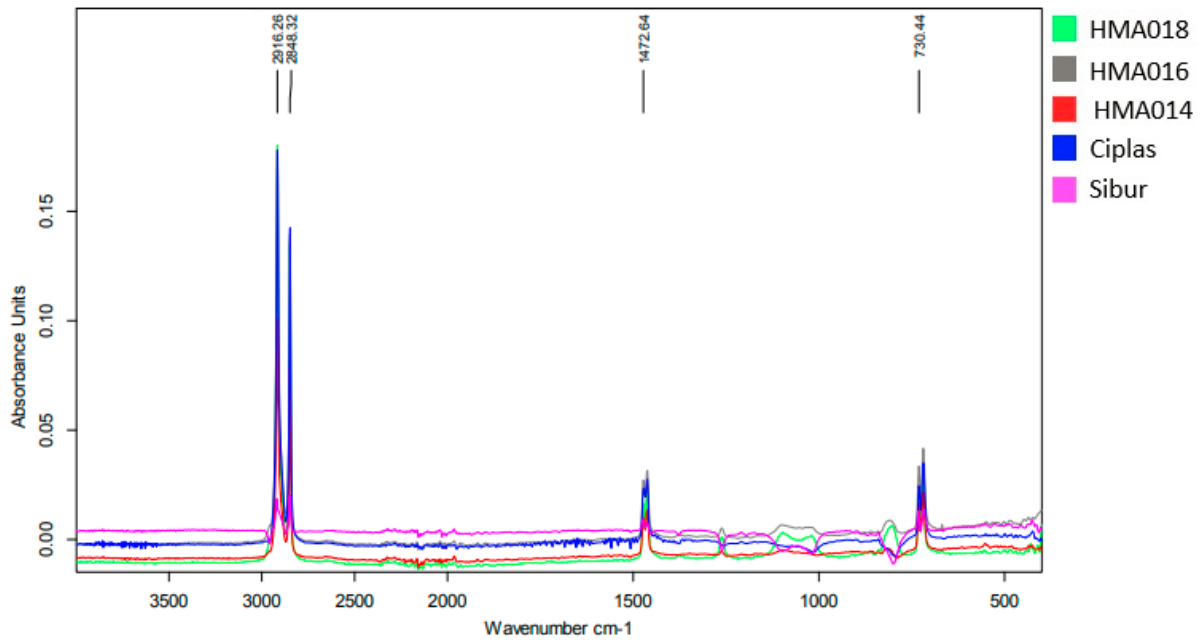

Figure 3. 8 *FTIR spectra of HDPE grades HMA018 (green), HMA016 (grey), HMA014 (red), Ciplas (blue), and Sibur (pink).*

3.2 Soxhlet Extraction of Additives

Soxhlet extraction is an efficient technique for extracting partially soluble impurities from an insoluble sample. However, it requires long extraction times and large volumes of solvent are needed.[131] Although other solvent extraction methods, such as supercritical fluid and microwave assisted extraction have shown better recovery rates in less time, soxhlet extraction has the advantage of being inexpensive and requiring minimal equipment.[132,133]

Preliminary soxhlet extraction experiments were performed to identify additives in HDPE grades and technique drawbacks to improve extraction parameters for forthcoming experiments. The method was partially adapted from Lehotay et al.[134] The total amount of extracts and their descriptions are shown in (**Table 3. 2**).

ExxonMobil was contacted to find out the type and concentration of additive formulations in their HDPE grades, however, this information was not disclosed. The concentration of additives in the HDPE grades are therefore unknown, and a yield could not be calculated.

During the first two runs, a colour difference between the two different solvents extractions was noticed. The chloroform extracts displayed a red/pink hue, meanwhile the hexane solutions were colourless (**Figure 3. 9**). However, during the second run, the stop-corks were changed from red rubber

suba-seals to glass stoppers. Once this change was made the red colouring was no longer visible after extraction, meaning chloroform was likely degrading the rubber and extracting the pigments. Later, methanol was added to the initial pink $CHCl_3$ solution and precipitation was observed alongside turning colourless.

Table 3. 2 *Total amount of samples/impurities extracted in grams from different HDPE grades via soxhlet extraction using chloroform and hexane consecutively at 110 °C and 250 RPM.*

HDPE Grade	Chloroform Extraction (g)	Hexane Extraction (g)	Total extracts (g)	Comments/Notes
HMA014	0.327	0.161	0.448	Formation of white ring on bottom of round bottom flask (RBF) following $CHCl_3$ extraction. Small specs of white residue were in RBF following hexane extraction.
HMA016	0.048	0.159	0.207	Small volume of clear liquid residue in RBFs after both extractions.
HMA018	0.338	0.180	0.518	Colourless liquid present after $CHCl_3$ extraction. Oily residue was present following the hexane extraction and rotavap.
Sibur	0.213	0.117	0.330	White crystalline residue formed after $CHCl_3$ extraction (**Figure 3. 9a**). Oily residue left in RBF following hexane extraction and rotavap.
Ciplas	0.206	0.215	0.421	No visible product in RBF after $CHCl_3$ extraction. Colourless liquid following hexane extraction.

The quantity of extracted products was minimal, especially following filtration. HDPE pellets are commonly ground up into powder to maximise the molecular interface.[135,132,134] This is largely due to the small surface area of HDPE pellets which limits solvent penetration and diffusion. The crystallinity and linear structure of HDPE hinders the solvent from penetrating the matrix.[131] In this case, extraction was performed on pellets. As a result, low recovery rates were obtained. Additionally, the filtration method used limited the yield due to multiple sample transfers. Which could have been simplified by filtering the solvent first, and then evaporating via rotavap which minimises intermediate steps. Additionally, at temperatures below 110 °C there was not enough heat to initiate reflux, causing the solvent ($CHCl_3$) to be stuck in the main chamber of the soxhlet apparatus and not cycle through the

siphon. Temperatures higher than 110 ^{o}C with greater RPM (>200) increased the kinetic energy of the system and allowed faster extraction cycles.

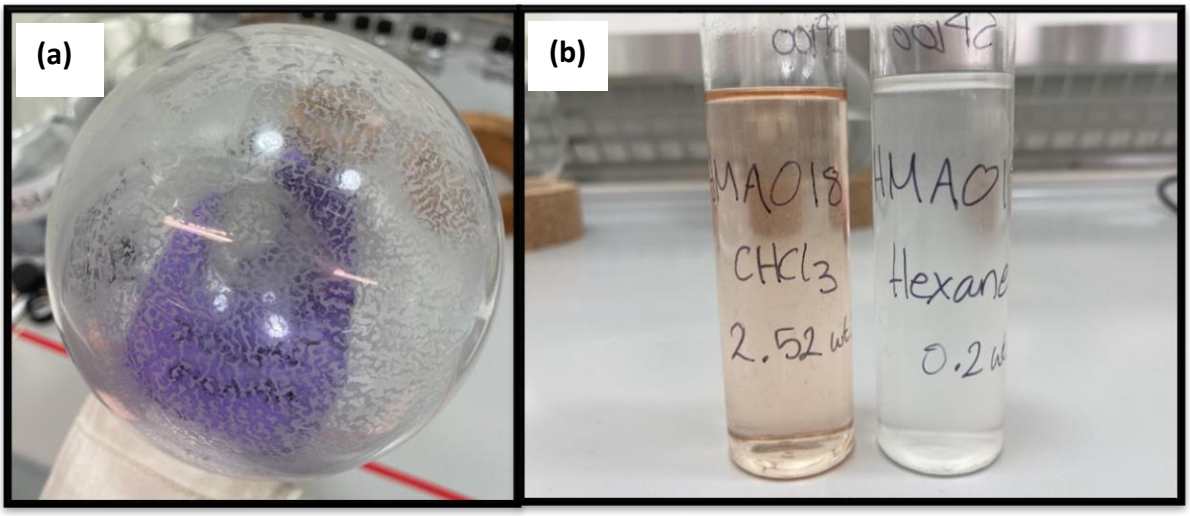

Figure 3. 9 *Images of (a) white crystallised residue after soxhlet extraction at 110^{o}C and 250 RPM of Sibur using chloroform and (b) HMA018 extract re-dissolved in chloroform (left) and hexane (right) following soxhlet extraction.*

As HMA018 had the highest extraction yield, the resulting products were analysed using FTIR to investigate the presence of additives. No peaks were seen in the products from hexane extraction, however an FTIR spectra was obtained for products from chloroform extractions (**Figure 3. 10**). The resulting spectrum showed evidence of residual HDPE, demonstrated by the peaks at around 2900 cm^{-1} (C-H stretch), 1400 cm^{-1} (C=C vibration) and 700 cm^{-1} (C-H bend). The peak around 1300 cm^{-1} could likely be due to methyl side chains, which was also seen in the spectra of HDPE grades (**Figure 3. 8**) but could not be resolved due to baseline distortion. Future work will focus on analysing these samples using high-pressure liquid chromatography (HPLC) coupled with mass spectroscopy (MS) as it is a more sensitive technique.[136] FTIR has limitations for materials with weak infrared absorption or overlapping spectral bands of the trace material with the major component, in this case the overlap of additive bands with HDPE oligomers.

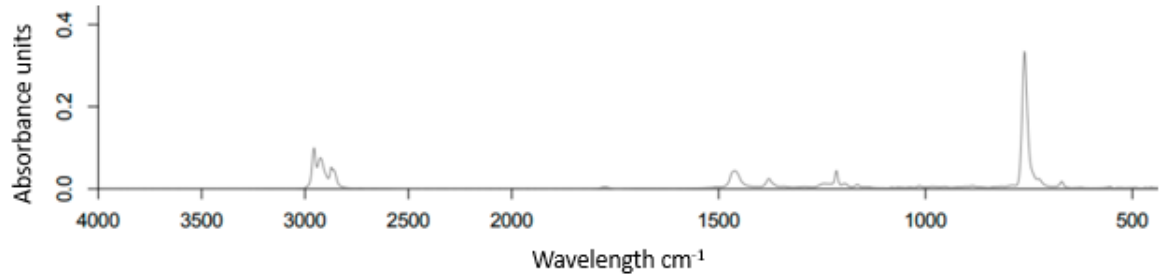

Figure 3. 10 *FTIR absorbance spectrum of impurities extracted from HDPE grade HMA018, obtained under soxhlet extraction using chloroform at 110 °C and 250 RPM.*

To increase the surface area and reduce particle size of the HDPE pellets, the HDPE samples were cryomilled for Soxhlet extraction. At cryogenic temperatures below T_g of HDPE, the polymer pellets become brittle with a uniform particle size during milling.[137] At elevated temperatures the pellets are bent and cannot be fractured due to the amorphous phases. Following cryogenic milling, the surface area of HDPE was successfully increased and the HDPE pellets were reduced to a powder (**Figure 3. 11**). It is hypothesised that higher extraction yields will be obtained with smaller particle size due to shorter diffusion distances. However, due to time limitations the powdered HDPE could not be utilised for soxhlet extraction.

Figure 3. 11 *White virgin HDPE pellets of HMA018 before (left) and after (right) cryogenic milling at 25 Hz.*

Considering that the concentrations of the additives are less than 0.2 wt. % (with respect to the polymer matrix), high extraction yields remain elusive. Therefore, longer extraction time, larger sample and smaller particle size are required to achieve detectable concentrations of additives. Even so, protocols for these techniques have been established and optimised for future studies. This data can be utilised to improve reaction conditions and extraction yields of additives to determine the influence of stabilisers on the mechanical recycling of HDPE.

3.3 Mechanical Recycling of HDPE

Mechanical recycling was simulated through 5 extrusion cycles of HDPE grades from ExxonMobil (HMA014, HMA016 and HMA018). The extrusion conditions required to successfully process HDPE varied between grades, and the lowest possible temperatures and RPM were used to minimise thermo-mechanical degradation. HMA014 required a temperature range of 180-230°C through the extruder barrel to obtain a continuous flow of extrudate without air bubbles. The RPM was set to 300 and the torque response ranged from 2.5-3.8 Nm. Meanwhile, a temperature range of 150-200°C was sufficient for HMA016, with an RPM of 200 and a lower torque response range of 2.1-2.7 Nm. HMA018 required slightly lower temperatures ranging from 150-180°C with the same RPM and similar torque response as HMA016. The torque response was directly proportional to the RPM and feed rate. At higher feed rates and lower RPM the torque response increased due to more volume and less shear in the barrel. The higher torque response and RPM required to process HMA014, opposed to HMA016 and HMA016 support that polymer grades with low MFI have higher SME (**Equation 1. 2**) and consume more mechanical energy for processing during recycling. This is because low MFI grades have higher viscosity, requiring more shear force to enable flow in the extruder barrel. Higher temperatures can lower viscosity, but this also increases thermal degradation. Meanwhile RPM could be increased to improve material flow, but this may increase mechanical degradation due to high shear rates. Alternatively, lubricants could be used to increase the MFI and increase extruder throughput, yet this could impact the melt strength of the polymer.[138]

3.3.1 Colour Measurements

After the first recycling cycle the polymers began to discolour (**Figure 3. 12**). Discolouration is an inevitable outcome of extrusion due to oxidative degradation, particularly due to phenolic antioxidant or flame retardants in the material.[139] Although phenolic antioxidants are crucial for scavenging radical peroxides, it also results in discolouration due to the reaction products from phenolic antioxidants and OH groups.[140,141] During such oxidation reactions quinones are formed which gives a yellow tint to the polymer.[142] As such, a linear correlation should be seen between the yellowness index (YI) and concentration of stabilisers that react during processing. [143,96,109,140]

Figure 3. 12 *Colour change with respect to extrusion cycles (virgin to cycle 5 from left to right) of HMA018 (top), HMA016 (middle) and HMA014 (bottom). The colour change is represented with pellets on the left half, and injection moulded dumbbells on the right half of the figure.*

The YI for all 3 HDPE grades increase with extrusion cycles and is most pronounced in HMA016 (**Figure 3. 13**). Note that negative YI values denote blue discolouration.[144] Therefore, the departure of YI towards more positive values indicates that the polymers are becoming more yellow and less blue with each recycling cycle. Both HMA014 and HMA018 have large deviations on cycle 2 which affects the linearity of the trend.

The colour change, *ΔE*, is greater for HMA016 (19.22), followed by HMA014 (11.49) and HMA018 (1.78). Although HMA014 was processed under higher temperatures and shear, these results may indicate that colour change and YI is irrespective of processing conditions and MFI of HDPE. These results do not support the hypothesis of high shear rates and temperatures causing more discolouration, and may suggest that temperature and shear rates do not influence the rate of stabiliser reactions with oxygen that form chromophores such as quinones. However, the data is not conclusive enough. Measurements of YI were only carried out once due to time limitations, therefore further repeats are necessary to confirm results and reduce errors.

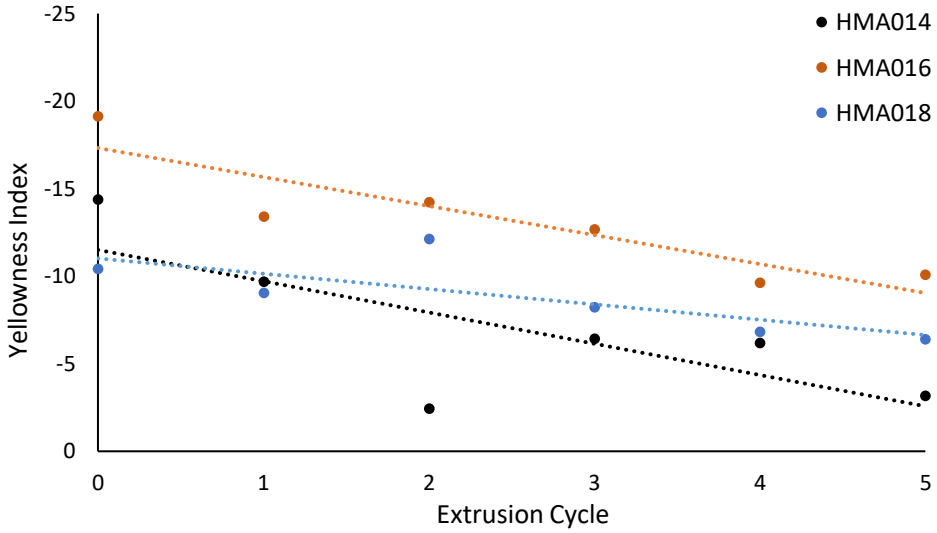

Figure 3. 13 *The change in yellowness index of HDPE grades with respect to extrusion cycles. The R^2 values for HMA014, HMA016 and HMA018 are 0.57, 0.82 and 0.56, respectively.*

3.3.2 Rheological Properties

Understanding rheological behaviour of HDPE provides insights into change in material topology as a result of recycling. Small changes in the polymer structure such as MW and branching have a significant impact on processing and recycling of the polymer melt.[145]

Complex viscosity of recycled HDPE grades decrease with increasing angular frequency (**Figure 3. 14**). The non-Newtonian behaviour i.e. shear thinning properties are seen due to the disentanglement of polymer chains under shear stress. At rest, the molecular chains are entangled and randomly orientated, but with increasing shear rate the polymer chains disentangle and align along the direction of shear.[146] This gives rise to greater free volume and less molecular interactions, therefore polymer chains can move more freely and viscosity decreases.

The viscosity of the material at the extruder speed was estimated using the equation below:

$$\text{Rad s}^{-1} = \frac{\text{RPM}}{60} \times 2\pi \qquad \textbf{(3. 2)}$$

Therefore, at 200 RPM the angular frequency will be 20.9 ≈ 25 rad/s. Understanding the melt behaviour of HDPE at 25 rad/s will reflect the impact of processing conditions in the extruder.

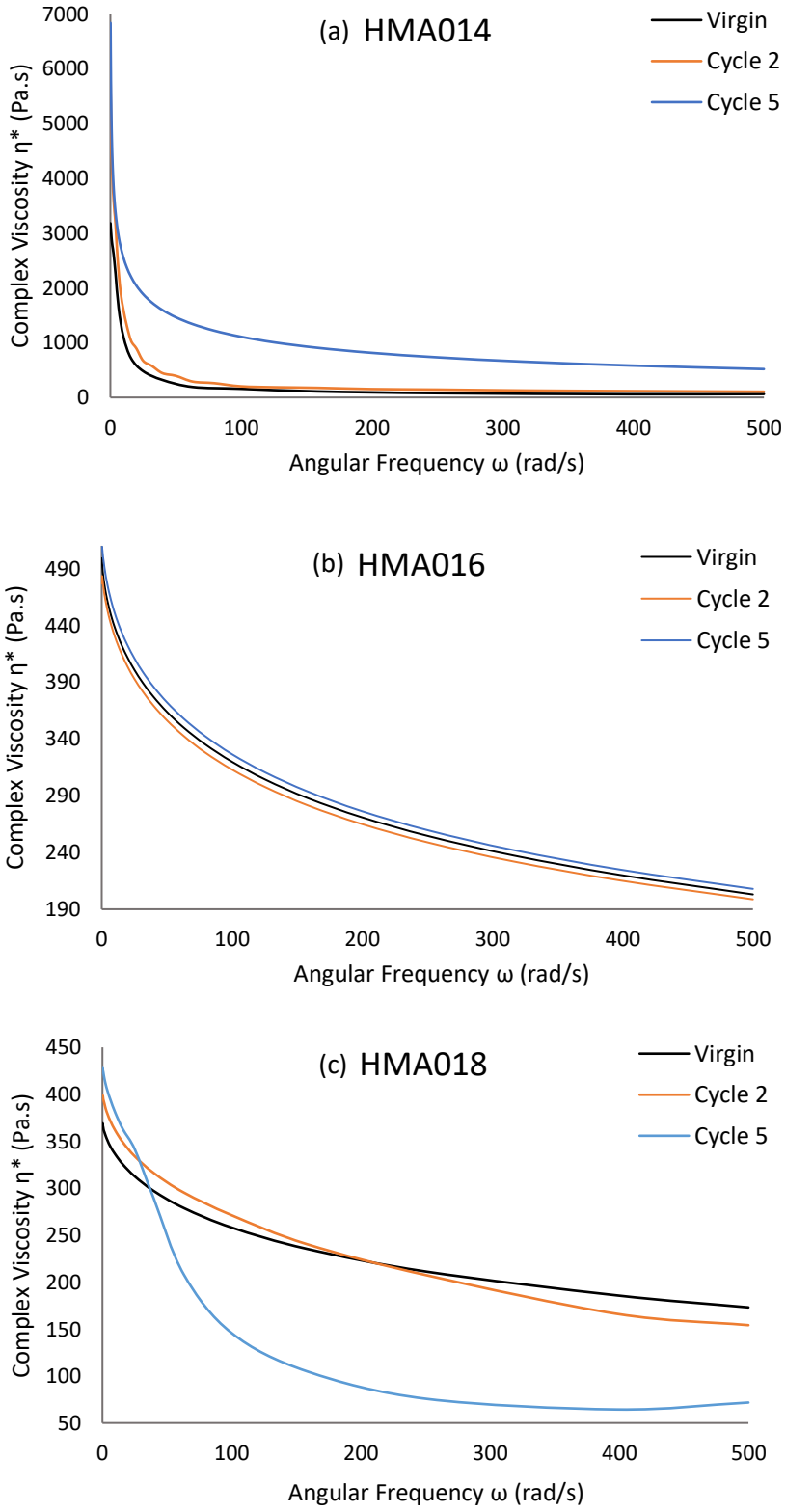

Figure 3. 14 *Decrease in complex viscosity (η*) with angular frequency (ω) for HDPE grades (a) HMA014, (b) HMA016, and (c) HMA018. Viscosity measurements were conducted on HDPE pellets through a frequency sweep at 180 °C.*

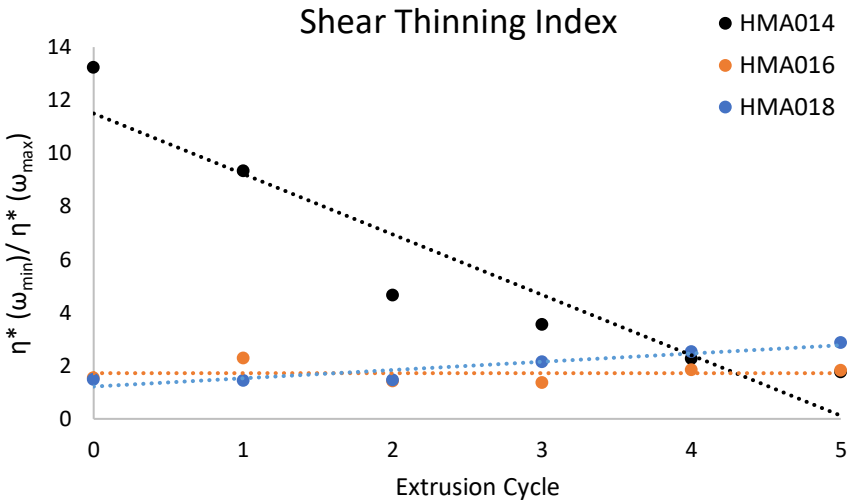

Figure 3. 15 *The variations in shear thinning index with respect to extrusion cycles. The shear thinning index decreases for HMA014 (R^2 = 0.84), does not change for HMA016 ($R^2 \approx 0$) and increases for HMA018 (R^2 = 0.88) over 5 recycling cycles. The shear thinning index was calculated by taking the ratio of complex viscosities at 0.1 rad/s and 100 rad/s. Viscosity was measured on HDPE pellets through frequency sweeps at 180 °C.*

Polymers with a broad MWD tend to thin more at lower shear rates.[75] Additionally, for polymers with long relaxation times shear thinning also occurs at low shear rates.[147] As seen in **Figure 3. 1** and **Figure 3. 14**, HMA014 has a more rapid onset in shear thinning properties than the other HDPE grades. This could suggest that HMA014 may have a broader MWD and longer relaxation time than the higher MFI grades, however SEC and further rheology measurements are required to confirm this.

The intensity of shear thinning can be calculated by obtaining the ratio of frequencies. In this case, the ratio between 0.1 and 100 rad/s was used to give a trend in shear thinning properties (**Figure 3. 15**). There is no change in shear thinning index for HMA016, a marginal increase for HMA018 (R^2 = 0.88) and a significant decrease for HMA014 (R^2 = 0.84). This means that HMA018 is becoming more shear thinning, whereas HMA014 is becoming shear thickening when recycled. The amount of energy required to process a polymer at a constant MW is proportional to its shear thinning properties.[75] The degree and onset of shear thinning differs between the polymer grades and are qualitatively related to MWD.

As expected, HMA014 has the highest complex viscosity, followed by HMA016 and then HMA018 (**Figure 3. 16**). This is consistent with their MFI, in which HMA014 has the lowest flow rate (4.0 g/10min) followed by HMA016 (20 g/10min) and HMA018 (30 g/10min), supporting the expectations that greater MW polymers have higher viscosities.

HMA014 has a large increase in complex viscosity between recycling cycles when analysed at high angular frequencies (25 rad/s). However, at low angular frequency (0.1 rad/s) there is a significant

decrease in viscosity (**Figure 3. 16**). This is unusual and could indicate that the chain structure is behaving differently when measured under different shear rates.

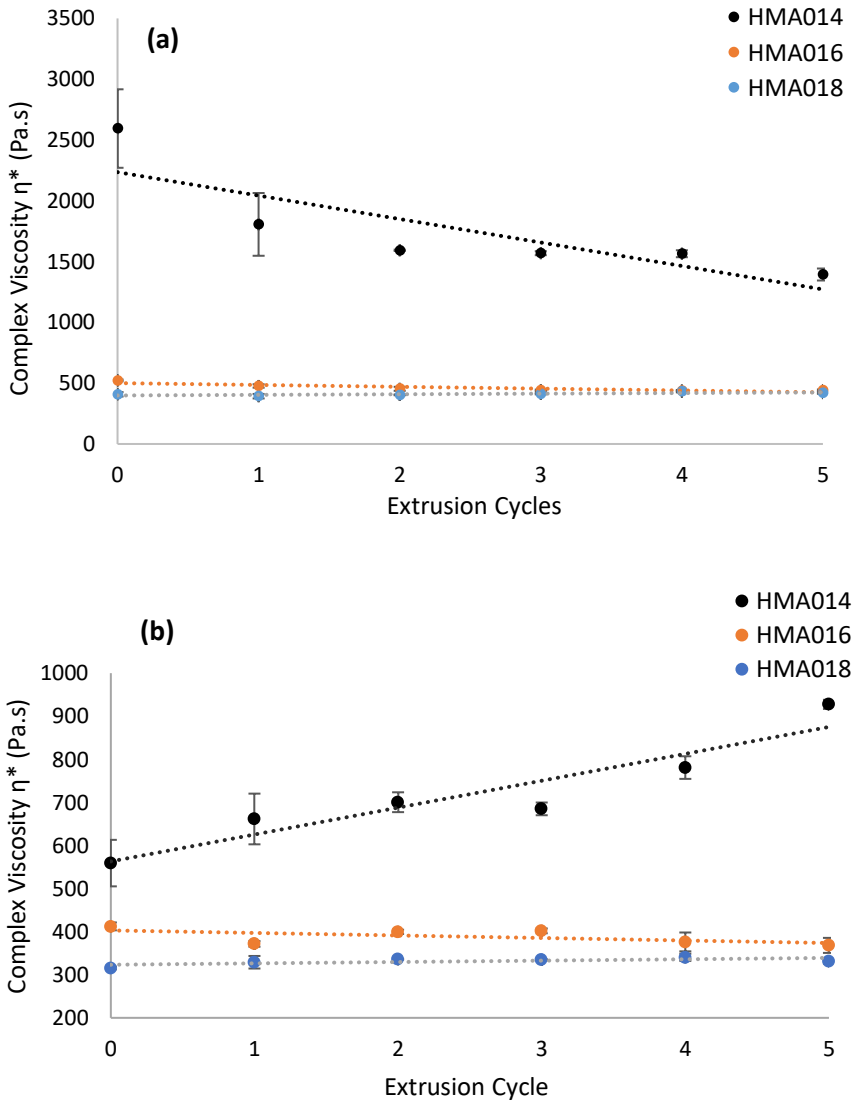

Figure 3. 16 *The changes in complex viscosity (Pa.s) of HDPE grades at (a) 0.1 rad/s and (b) 25 rad/s over five extrusion cycles. Viscosity, η*, was obtained through rheology measurements on HDPE pellets at 180 °C. The R^2 values for figure (a) are 0.65, 0.75 and 0.91 for HMA014, HMA016 and HMA018, respectively. For figure (b) the R^2 values are 0.88, 0.35 and 0.48 for HMA014, HMA016 and HMA018, respectively. Standard errors for η* were calculated over three tests.*

This is hypothesised to be influenced by the polymer relaxation times and elasticity, or perhaps due to simultaneous cross-linking alongside chain scission of the recycled samples. During standard extrusion, oxygen present in the air can react with the polymer chains to form macro-radicals, which in turn react with terminal double bonds present in other HDPE polymer chains to form cross-links.[91] At high shear rates the cross-links are maybe becoming more entangled and are inhibiting alignment in direction of shear. Further analysis of relaxation times using rheology may bring more clarification.

When the data from **Figure 3. 16** is magnified (**Appendix 7.1.1**), the viscosities between recycling cycles are fluctuating. This may confirm that chain scission and branching are happening simultaneously. However, these fluctuations are minimal (<9 %) with large error bars. On a larger graphical scale, there is an overall increase in viscosity for HMA018 which is more prominent at low shear rates. As mentioned previously (**Section 1.6.1.3**), the MW is proportional to the viscosity at low shear rates. The data can suggest that chain branching is becoming more pronounced for HMA018 with each recycling cycle. Shorter chains are less susceptible to shear stress during mechanical processing and more prone to chain branching due to readily accessible terminal groups. With more chain branching, the viscosity increases as bulky polymer chains have reduced ability to flow past each other. Contrarily, HMA016 shows decreasing viscosity with recycling at low shear rates (**Figure 3. 16**). This could suggest that chain scission is more pronounced. With the increasing number of shorter chains, plasticizing effects can be seen because shorter chains are more mobile which decreases the viscosity. At high shear rates (25 rad/s), there is no evident change in viscosity for HMA016 or HMA018.

An indicator of the change in material elasticity is the loss angle, tan δ, which can be described using the ratio between storage (G'), loss (G") and complex modulus (G*) as shown in **Figure 3. 17**. This relationship can be illustrated using Pythagoras theorem:

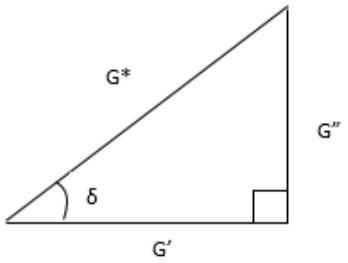

Figure 3. 17 *Illustration of the relationship between storage (G'), loss (G") and complex modulus (G*) through a right angle triangle representing Pythagoras theorem.*

Where $(G^*)^2 = (G')^2 + (G'')^2$, therefore, $Tan\ \delta = \frac{G''}{G'}$ **(3. 3)**

This ratio is useful for identifying the overall viscoelasticity of the polymer. If tan δ is < 1, then the material is more elastic than viscous, and if tan δ is > 1, the material is more viscous than elastic .[148] The greater the tan δ, the more energy dissipation potential of the material. The mechanical characteristics of viscoelastic polymeric materials are in between those of a viscous liquid and elastic solid.[149]

All three HDPE grades display viscoelastic behaviour. HMA018 (R^2 = 0.93) and HMA014 (R^2 = 0.84) shows a decrease in tan δ meaning that it is becoming more elastic, whereas there is nominal change in viscoelasticity for HMA016 (**Figure 3. 18**). It can be assumed that overall, the material elasticity for HMA014 and HMA018 increases with recycling, which can be a result of cross-linking interactions that can overcome mechanical perturbation. HMA014 is the most elastic out of the three grades, meaning it can more readily return to its original structure once load/stress is removed. The high MW chains and entanglement kinetics may have influence over this property, as the entangled chains can stretch and return to their original configuration more readily without the breakage of intermolecular bonds.

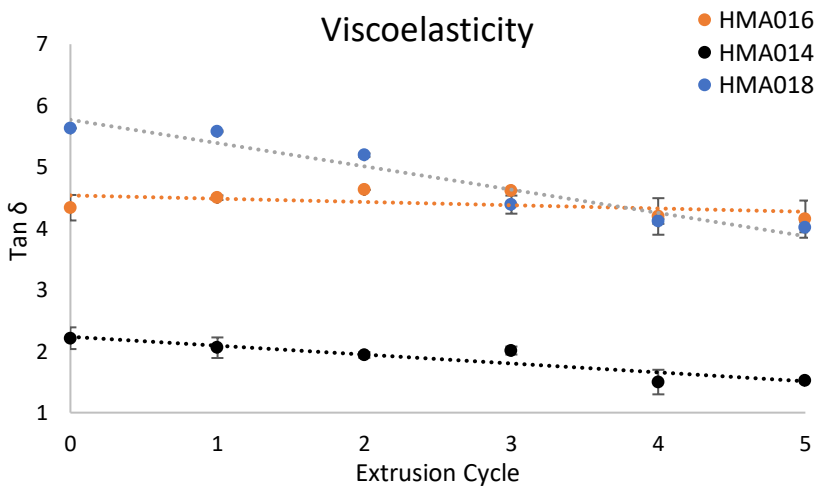

Figure 3. 18 *The change in tan δ values over five extrusion cycles. Tan δ decreases for HMA014 (R^2 = 0.84), does not change for HMA016 (R^2 = 0.23) and decreases for HMA018 (0.93). Tan δ was obtained through the ratio of loss (G") and storage (G') modulus calculated at 25 rad/s through rheology measurements at 180 °C. Standard errors were calculated over three tests.*

3.3.3 Thermal properties and Crystallinity

From the technical data sheet provided by the polymer manufacturer, the glass transition temperature of HMA018 is approximately -130 °C. Consequently, the T_g could not be obtained as the

DSC was limited to -80 °C.[150] The T_g is dependent on the amorphous regions of the polymer, and therefore HDPE has very low T_g due to its high crystallinity.

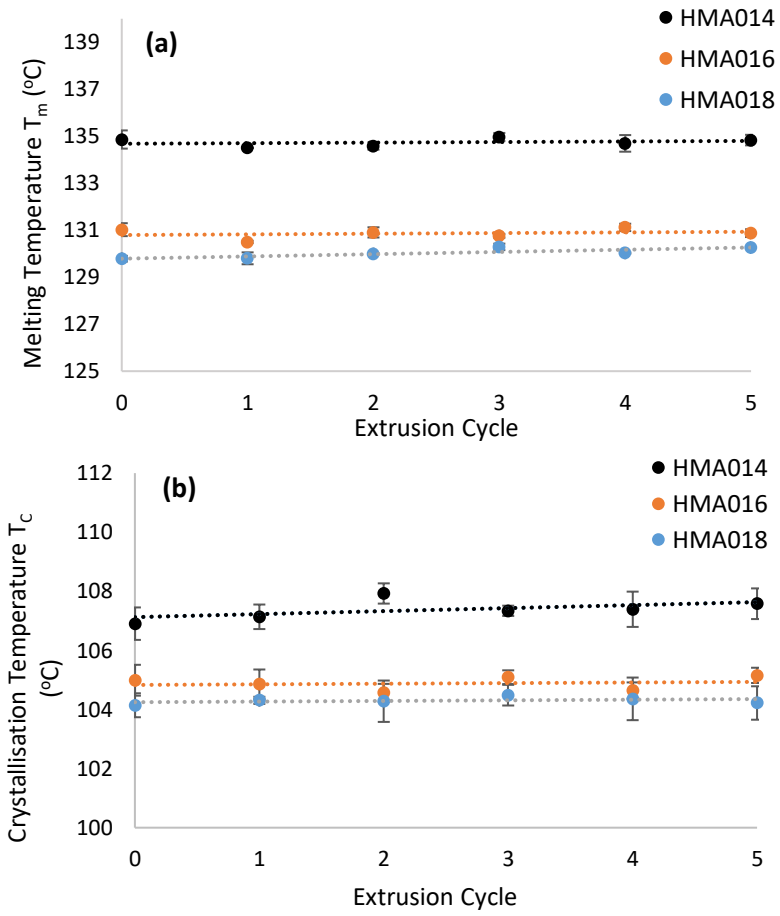

Figure 3. 19 *The (a) melting, T_m and (b) crystallisation temperatures, T_C, over five extrusion cycles of HDPE grades showing negligible variability. The R^2 values for T_m are 0.064, 0.057 and 0.68 for HMA014, HMA016 and HMA018 respectively. The R^2 values for T_c are 0.29, 0.025 and 0.11 for HMA014, HMA016 and HMA018, respectively. Standard errors for T_m and T_c were calculated over three tests.*

There are no significant changes in crystallisation and melting temperature for the HDPE grades when recycled 5 times (**Figure 3. 19**). However, there is a slight increase in T_m for HMA018 which can be attributed to its increasing crystallinity (**Figure 3. 20**). This is because more energy is required to overcome the intermolecular bonds to transition from an ordered crystalline phase to a disordered amorphous phase. HMA014 has the greatest T_m and T_C, followed by HMA016 and HMA018. This trend is also observed in their degrees of crystallinity and MFI, with HMA014 being the most crystalline (lowest MFI), followed by HMA016 and HMA018 (**Figure 3. 20**). The changes in % crystallinity are minimal with fluctuations of less than ± 1.5 % between cycles, and by cycle 5 both HMA016 and HMA018 have similar crystallinities.

The slight increase in % crystallinity for HMA018 is tentatively attributed to chain scission. As the MW decreases, chain mobility increases and crystalline growth is promoted. This is because the amorphous phase of the polymer is attacked more readily during thermo-oxidative degradation, leaving behind crystalline domains which act as nucleation points. As such, growth of the crystalline phase is observed with increasing recycling cycles. The low MFI grades (HMA014 and HMA016) have better crystallinity retention opposed to the high MFI grade, HMA018. This partially supports the hypothesis, showing that low MFI grades have less variations in properties when recycled. However, with large error bars there is overlap between % crystallinity values for HMA016 and HMA018. Some literature report and increase in crystallinity for HDPE with recycling cycles, whereas others report a decrease or no change.[70,97] With seemingly similar methodologies, the variations in literature are likely due to differences in HDPE grades. The different MWDs of the grades will influence the rate and frequency of chain scission and cross-linking, which in turn will affect the orientation and packing density of polymer chains. Consequently, mechanical properties are also likely to be affected because intermolecular bonding is more prominent in the crystalline phase.[151]

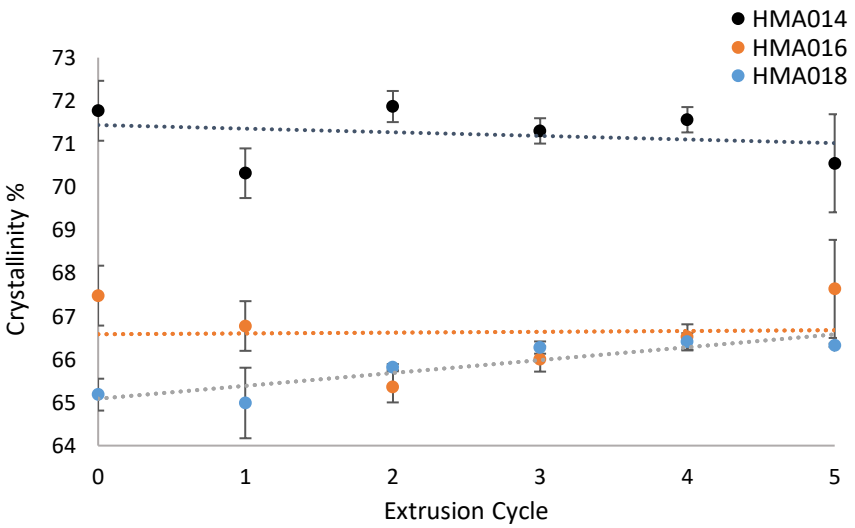

Figure 3. 20 *Change in crystallinity of HDPE grades obtained through DSC measurements as a function of five extrusion cycles. The % crystallinity does not change for HMA014 (R^2 = 0.059) and HMA016 (R^2 = 0.0017), but increases for HMA018 (R^2 = 0.82). Standard errors for % crystallinity were calculated over three tests.*

3.3.4 Mechanical Properties

Mechanical properties of the HDPE grades with respect to extrusion cycles were measured, and values for Young's Modulus (E), Yield Strength (σ_m) and Strain at Break (ε_b) were obtained. The specimens

measured were prepared by injection moulding (**Section 2.2.2**). This process involves both heat and shear, therefore is likely to result in further degradation of the materials.

Both E and σ_m exhibited similar trends (**Figure 3. 21**). There is no significant change in E for HMA014, a marginal decrease for HMA016 and an increase for HMA018. Between recycling cycles 0-5, ε_b is greatest for HMA016 (~800-1000%), followed by HMA018 (~500-900%) and HMA014 (~220-420%).

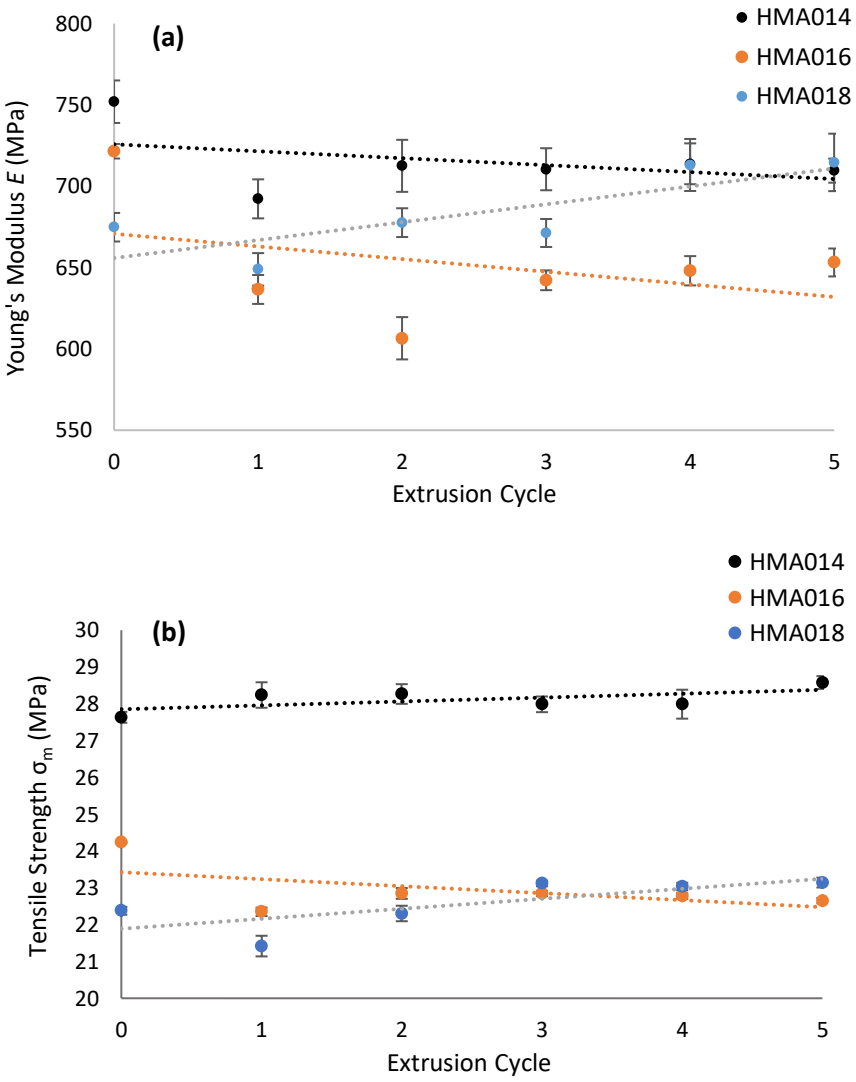

Figure 3. 21 *Young's Modulus, E (a) and tensile strength, σ_m (b) as a function of five extrusion cycles, obtained through tensile testing on injection moulded dumbbells at a rate of 50 mm/min. The R^2 values for Young's Modulus are 0.16, 0.15 and 0.64 for HMA014, HMA016 and HMA018, respectively. The R^2 values for tensile strength are 0.38, 0.29 and 0.57 for HMA014, HMA016 and HMA018, respectively. Standard errors for E and σ_m were calculated over five tests.*

An increase in Young's Modulus (YM) indicates the material is becoming more brittle (**Figure 3. 21a**), which in turn translates to a decrease in elasticity. This is mirrored by the decrease in ε_b for HMA018 in (**Figure 3. 22**). The patterns in strength and YM are similar to the % crystallinity of the grades. The

YM of HMA018 increases (5.2 %) because the crystallinity increases (**Figure 3. 20**). Higher % crystallinity results in greater density of the polymer, therefore, the lack of voids and pores in the polymer matrix gives a close-packed structure, increasing secondary bonding interactions and material stiffness. Meanwhile, the strain at break, ε_b decreases (52 %) as a result of increasing stiffness and % crystallinity. Due to chain entanglement taking place in the amorphous phase, the increasing crystallinity limits the degree of entanglement, resulting in less extension before the breaking strain is reached. Therefore, ε_b decreases with each recycling cycle of HMA018 as chain lengths become shorter and the magnitude of secondary bonding chain interactions decrease.

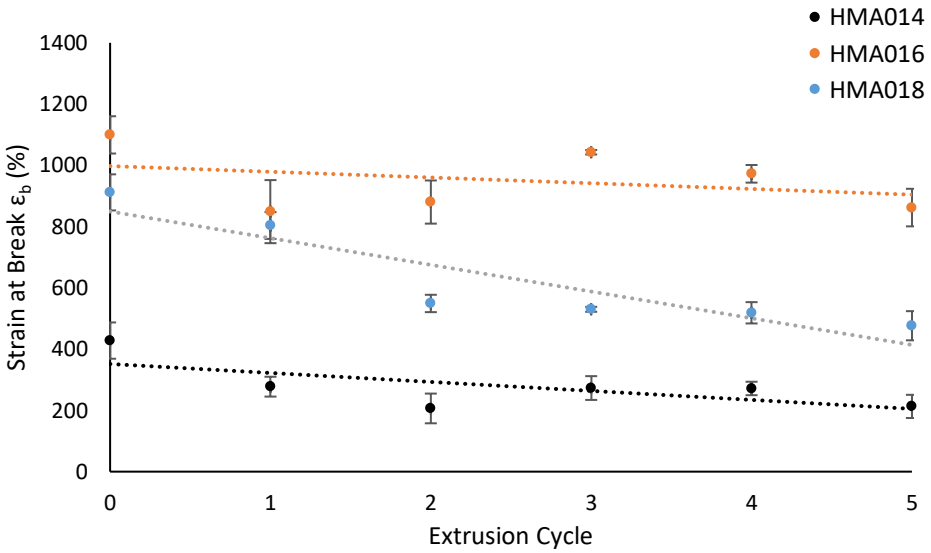

Figure 3. 22 *Strain at break, ε_b (%) as a function of five extrusion cycles, obtained through tensile testing on injection moulded dumbbells at a rate of 50mm/min. ε_b shows minimal changes for HMA014 (R^2 = 0.11), a very small decrease for HMA016 (R^2 = 0.5) and a significant decrease for HMA018 (R^2 = 0.82). The standard errors for ε_b were calculated over five tests.*

There are nominal changes in ε_b for HMA016 and HMA014 (**Figure 3. 22**). Considering the large error bars for HMA016, it could be said that ε_b stays relatively constant. Overall, HMA014 shows the least change in mechanical properties during repetitive recycling cycles. These results support the hypothesis and show that low MFI grades are better at retaining mechanical properties when recycled. This could be attributed to the strong intermolecular interactions and entanglement kinetics of long chain polymers.

There is a direct relationship between MW and mechanical properties. The tensile strength is related to the MW using the following equation:

$$\sigma = \sigma_{\infty} - \frac{A}{M} \qquad \textbf{(3. 4)}$$

Where σ_∞ is the tensile strength of the polymer with a molecular weight of infinity. A is a constant and M is the MW of the polymer.[151] At low MW, the chains can move more readily due to weak Van der Waals forces, resulting in low strength irrespective of crystallinity. In the case of higher MW (lower MFI) grades, the long chains are entangled and intermolecular bonding becomes more significant. Tensile testing on further grades including Sabir and Ciplas would further support the hypothesis and improve reliability.

Values for YM have relatively large error bars. The variability in YM during tensile testing could be a result of fluctuations in dwelling and temperature during injection moulding. The probability of thermo-oxidative degradation is increased when the polymers are exposed to high temperatures for long time periods. As such, it will be preferable to improve consistency between HDPE samples through directly extruding into blown films without intermediate processing steps for mechanical testing.

3.3.5 FTIR Analysis

FTIR was conducted to analyse the effects of degradation and variations in structure change between HDPE grades. The characteristic FT-IR HDPE bands are located at 2916 cm^{-1} (asymmetric C-H stretch), 2848 cm^{-1} (symmetric C-H stretch), 1473 cm^{-1} (C=C vibration) and 730 cm^{-1} (C-H bend). The FTIR spectra of recycled HDPE grades (**Figure 3. 23**) do not show significant differences with consecutive recycles. Additionally, carbonyl peaks were expected in the 1700 cm^{-1} region due to oxidative degradation, but such peaks were not present. This is likely because the sensitivity of FTIR is not high enough to detect carbonyls and degradation products in the HDPE matrix.[152] Although minor discrepancies can be seen in the 1300-1400 cm^{-1} region which could suggest chain branching, this may be due to baseline distortion. As mentioned previously (**Section 3.1.2**) Improved resolutions can be obtained by increasing the number of scans, using reflective mode measurements on pellets or transmission mode on thin films (<50 µm). The FTIR measurements were run on HDPE pellets which are too thick for transmission mode analysis.[130] Alternatively, attenuated total reflection (ATR) FTIR could be used. The carbonyl index (CI) can be calculated through the ratio of the band area attributed to carbonyl (C=O) group and the area of the band of the methylene group (CH_2).[130] The relative CI between recycling cycles will indicate the degree of oxidative degradation.

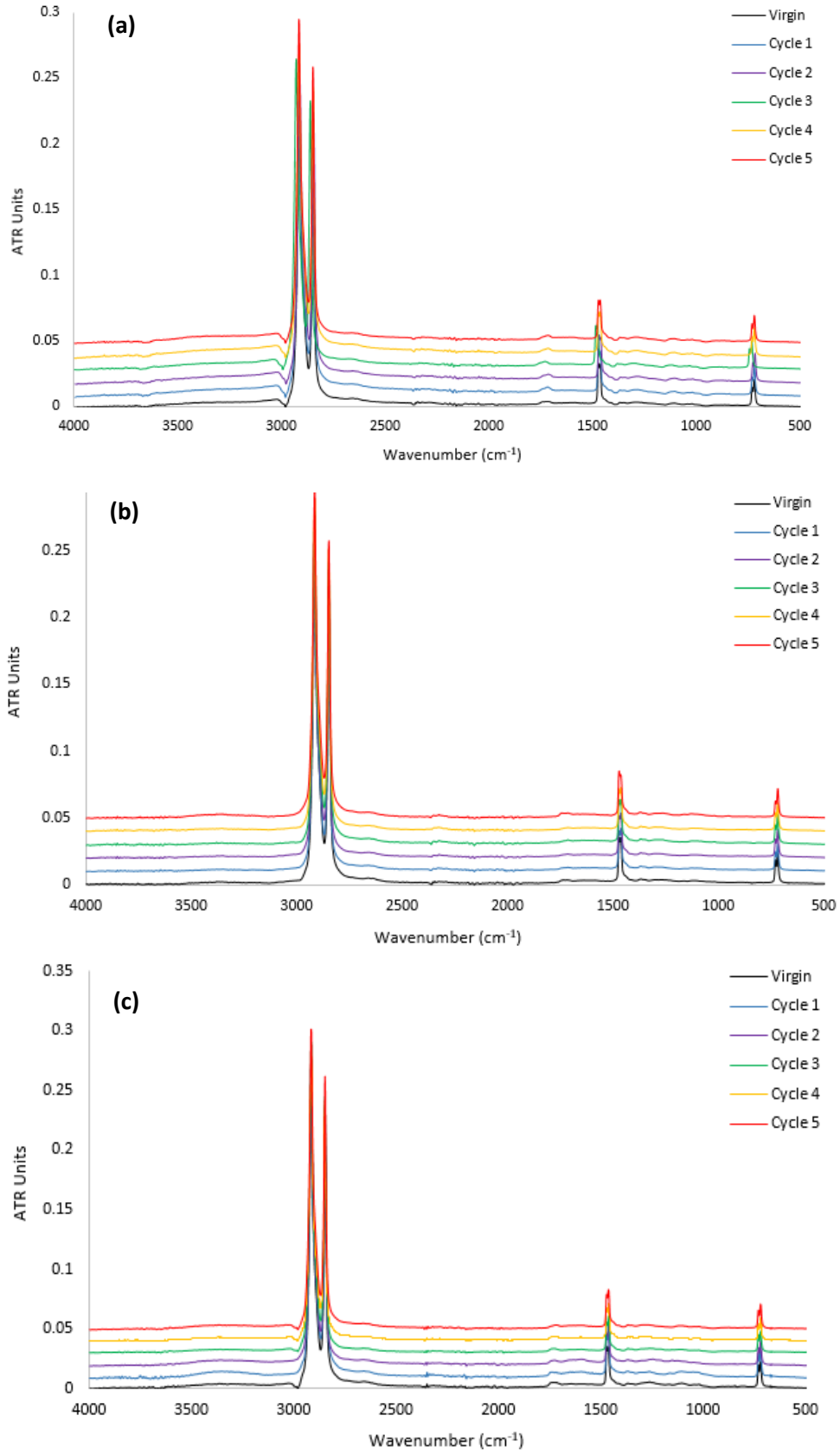

Figure 3. 23 *FTIR spectra of recycled HMA014 (a), HMA016 (b) and HMA018 (b). Five recycling cycles are shown on the spectra, from virgin to cycle 5.*

4 Conclusions

A foundation of data has been built on the property response of different HDPE grades (HMA014, HMA016, HMA018, Ciplas and Sibur) during mechanical recycling. The change in mechanical, thermal and rheological properties of three HDPE grades from ExxonMobil during mechanical recycling was explored and the degradation process was analysed. This research could be used in future to tailor HDPE materials to improve their recycling efficiency or predict the cycle after which HDPE will fail to recycle. Various trends and correlations between certain properties and the HDPE grades were confirmed. These results could mean that the behaviour of unknown HDPE grades during recycling could be predicted by knowing a single property such as the MFI. Through this, it can possible to predict whether a certain HDPE grade is suitable for recycling. However, it was found that correlations in properties are more significant between grades from the same manufacturers (ExxonMobil), and deviations were often presented when compared to different company grades (Sibur and Ciplas), bringing limitations to this theory.

Discolouration was significant during recycling and the yellowness index increased with each recycling cycle. The colour change was most pronounced for HMA016 ($\Delta E = 19.22$), followed by HMA014 and HMA018, which does not correlate with their MFIs, meaning that discolouration is unlikely to be influenced by processing conditions such as shear rate and temperature. It was found that mechanical recycling through five extrusion cycles had little effect on the thermal properties for all three grades of HDPE tested, although a slight increase (1.2 %) in % crystallinity for HMA018 was observed. Rheological measurements showed small fluctuations in viscosity between recycling cycles, supporting that simultaneous chain scission and branching of HDPE may be taking place.[98,92,91] However, these fluctuations were less than 9 %. On average, there were minimal changes in rheological properties for the high MFI grades (HMA016 and HMA018). Yet, the grade with the lowest MFI (HMA014) displayed unusual rheological properties when recycled. At high shear rates the viscosity increased between extrusion cycles, whereas at low shear rates the viscosity decreased. This suggests that the inherent chain structure is behaving differently when recycled under different shear rates.

On average, the tensile properties of HDPE grades were well retained when recycled. There was nominal changes in mechanical properties for HMA014. HMA018 showed a slight increase in Young's Modulus (5.6 %) and tensile strength (3.3 %), but a significant decrease in elongation at break (52 %). Meaning that recycling made the material more brittle and less ductile. A minimal decrease in YM and tensile strength was seen for HMA016, whereas the strain at break remained relatively constant. Overall, HMA014 displayed the least degradation during recycling cycles, which can be attributed to

having a lower MFI, higher MW and therefore stronger chain entanglement kinetics. The significant variations in viscosity for HMA014 may indicate branching and cross-linking effects during recycling. If this is the case, then it may be possible to improve the recycling quality of HDPE by incorporating chain extenders and cross-linkers during reactive extrusion, although this may affect the desired MFI of the material.

The correlation between mechanical, thermal and rheological behaviours of different MFI grades is not novel, but rather confirms the importance of such properties. It was examined that grades with lower MFI were likely to have improved mechanical behaviour. Furthermore, high crystallinity and density values corresponded to greater mechanical properties and viscosity. Although strong correlations were seen, Ciplas and Sibur don't follow the same MFI-dependent trends because they were synthesised by different manufacturers - likely to have been polymerised using different catalysts and co-monomers. The choice of catalysts and co-monomers will affect the MWD and chain structure of HDPE, which in turn will affect the degradation kinetics during recycling.

In order to achieve a greater understanding of the degradation behaviour of HDPE grades, soxhlet extraction was carried out to analyse the influence of additives on recycling. However, additives could not be detected from FT-IR and only oligomers could be seen. Low additive concentrations (< 0.2 wt. % with respect to the polymer matrix) and the dense linear structure of HDPE inhibits efficient soxhlet extraction. Solvent penetration was restricted due to the low surface area and high diffusion distances of the large HDPE pellets. Extraction efficiency would be improved by reducing particle size and it was shown that this could be achieved through cryogenic milling.

Overall, lower MFI grades performed better during recycling – suggested to be due to stronger chain entanglement kinetics. Further understanding of the behaviour of different HDPE grades under multiple extrusion cycles will elaborate the influence of MFI on degradation. This research could be expanded by exploring the influence of different Ziegler-Natta, metallocene or Phillips catalysts on the quality of HDPE recyclate due to their strong control over polymer MWD. This could also be expanded to a larger number of HDPE grades with the aim to develop a mapping system using a linear regression model, where the recycling prospects of unknown HDPE grades could be predicted. This area of research is necessary to enable and facilitate the development of a circular plastic economy.

5 Future work

The ultimate objective for facilitating a circular plastic economy is to mitigate degradation of plastic materials whilst extending lifetime as much as possible. Through analysing the degradation kinetics of different HDPE grades and the quality of recyclate, one can pinpoint advantages in properties which facilitate efficient recycling with minimal property loss. A baseline of research has successfully been developed, and it has been shown that low MFI grades are more suitable for recycling. To further support these findings, more HDPE grades need to be recycled and analysed. Although five recycling cycles of HMA014 showed good preservation of thermal and mechanical properties, the extrusion cycles need to be extended further to see when the material reaches its recycling limit. Further experiments and characterisations should entail thermogravimetric analysis to understand how thermal stability of HDPE grades are retained when recycled. Additionally, SEC such as gel permeation chromatography can determine the influence of MWD and dispersity on the degradation kinetics of HDPE to understand the MW influence on mechanical properties and processability. The processability and flow behaviour can be characterised through MFI testing. The FTIR spectra obtained in this project was not sufficient to observe degradation products or additives in virgin and recycled HDPE grades. This can be improved by using ATR-FTIR spectroscopy to observe the degree of oxidative degradation through measuring the carbonyl index. Alternatively, surface-enhanced Raman spectroscopy can be utilised to measure crystallinity and changes in intrinsic polymer structure. However, a fundamental understanding of the influence of polymerisation routes and catalysts on the recycling behaviour of different polymer grades is important. Through this, it could be possible to design or utilise specialised catalysts which yield favourable recycling qualities, such as bi-modal MWD with large MW fractions and low MFI. As such, future work in this field should entail the synthesis of HDPE using metallocene, Ziegler-Natta and Phillips catalysts, and then to analyse the degradation behaviour during mechanical recycling. The results could further aid catalyst selection and design for intended recycling use. However, a minimum yield of 1 kg of HDPE would be required to have a sufficient amount for five extrusion cycles, analysis, sample loss and compensation for errors.

Preliminary work has aided the design of an efficient soxhlet extraction experiment. Future work should entail cryogenic milling of HDPE pellets, followed by soxhlet extraction at 110 ^{o}C or higher for 24-48 hours with minimal sample transfer to increase yields. The additives can then be analysed through FTIR and nuclear magnetic resonance (NMR) to identify characteristic functional groups, and HPLC-MS for selective separation of extraction components such as oligomers, impurities and additives, followed by quantitative gradient analysis of retention times using additive standards. However, due to the possibility of a vast number of additives, it may be difficult to identify additives

through retention times of standards. Therefore, efficiency can be achieved by first identifying common functional groups through FTIR and NMR, and then selecting additive standards for HPLC which include similar chemical structures. This can narrow down the number of additive possibilities.

Additionally, to develop an effective mapping system of HDPE properties, further grades need to be analysed and recycled. Although correlation in thermal, rheological and mechanical properties is not novel, it could be beneficial and efficient to develop a mathematical model such as a multiple linear regression to predict the properties and potential degradation kinetics of a certain HDPE grade. The main drawback found is grades from different companies such as ExxonMobil and Ciplas do not follow similar trends. Therefore, independent models can be developed which can be categorised in to different suppliers. For example, by gathering a large database of HDPE grades from a specific supplier, and then mechanically processing a number of times, followed by processing analytical data and creating a linear regression model, the properties and recycling prospects of an unknown grade can potentially be obtained. Considering the proceeding plastic packaging tax, this could save valuable time and resources for companies and manufacturers on decision making, and choosing an effective HDPE grade which is recyclable and profitable.

Overall, this project has provided a fundamental insight to the recycling prospects of HDPE, contributing to the growing research in polymer processing to facilitate the adaptation of a circular plastic economy.

6 References

1 C. Rizan, F. Mortimer, R. Stancliffe and M. F. Bhutta, Plastics in healthcare: time for a re-evaluation, *J. R. Soc. Med.*, 2020, **113**, 49–53.

2 S. Ebnesajjad, in *Plastic Films in Food Packaging: Materials, Technology and Applications*, 2012, pp. 1–398.

3 K. Thirumaran, G. Balaji and N. D. Prasad, in *Sustainable urban architecture: select proceedings of VALUE*, 2020, p. 232.

4 Plastics – the Facts, An analysis of European plastics production, demand and waste data, *Assoc. Plast. manfacture*, 2015, 1–30.

5 L. Lebreton and A. Andrady, Future scenarios of global plastic waste generation and disposal, *Palgrave Commun.*, 2019, **5**, 1–11.

6 E. Elhacham, L. Ben-Uri, J. Grozovski, Y. M. Bar-On and R. Milo, Global human-made mass exceeds all living biomass, *Nature*, 2020, **588**, 442–444.

7 T. Hundertmark, M. Mayer, C. McNally, S. Theo Jan and W. Christof, How plastics waste recycling could transform the chemical industry - McKinsey & Company, https://www.mckinsey.com/industries/chemicals/our-insights/how-plastics-waste-recycling-could-transform-the-chemical-industry%0Ahttps://www.mckinsey.com/industries/chemicals/our-insights/how-plastics-waste-recycling-could-transform-the-chemical-industry#, (accessed 24 May 2021).

8 R. Geyer, J. R. Jambeck and K. L. Law, in *Science Advances*, American Association for the Advancement of Science, 2017, vol. 3.

9 R. Verma, K. S. Vinoda, M. Papireddy and A. N. S. Gowda, Toxic Pollutants from Plastic Waste- A Review, *Procedia Environ. Sci.*, 2016, **35**, 701–708.

10 A. Chamas, H. Moon, J. Zheng, Y. Qiu, T. Tabassum, J. H. Jang, M. Abu-Omar, S. L. Scott and S. Suh, Degradation Rates of Plastics in the Environment, *ACS Sustain. Chem. Eng.*, 2020, **8**, 3494–3511.

11 A. Banerjee and W. L. Shelver, Micro- and nanoplastic induced cellular toxicity in mammals: A review, *Sci. Total Environ.*, 2021, **755**, 142518.

12 C. Q. Y. Yong, S. Valiyaveettil and B. L. Tang, *Toxicity of microplastics and nanoplastics in Mammalian systems*, MDPI AG, 2020, vol. 17.

13 H. A. Leslie, M. J. M. van Velzen, S. H. Brandsma, D. Vethaak, J. J. Garcia-Vallejo and M. H. Lamoree, Discovery and quantification of plastic particle pollution in human blood, *Environ. Int.*, 2022, 107199.

14 A. Ragusa, A. Svelato, C. Santacroce, P. Catalano, V. Notarstefano, O. Carnevali, F. Papa, M. C. A. Rongioletti, F. Baiocco, S. Draghi, E. D'Amore, D. Rinaldo, M. Matta and E. Giorgini, Plasticenta: First evidence of microplastics in human placenta, *Environ. Int.*, 2021, **146**, 106274.

15 Z. Yuan, R. Nag and E. Cummins, Human health concerns regarding microplastics in the aquatic environment - From marine to food systems, *Sci. Total Environ.*, 2022, **823**, 153730.

16 M. C. Tanzi, S. Farè and G. Candiani, in *Foundations of Biomaterials Engineering*, Academic Press, 2019, pp. 3–103.

17 K. Ragaert, L. Delva and K. Van Geem, Mechanical and chemical recycling of solid plastic waste, *Waste Manag.*, 2017, **69**, 24–58.

18 A. Chruszcz and S. Reeve, *Composition of plastic waste collected via kerbside - Results of a waste compositional analysis of plastics at MRFs and PRFs*, 2018.

19 Z. O. G. Schyns and M. P. Shaver, Mechanical Recycling of Packaging Plastics: A Review, *Macromol. Rapid Commun.*, 2021, **42**, 2000415.

20 N. Singh, D. Hui, R. Singh, I. P. S. Ahuja, L. Feo and F. Fraternali, Recycling of plastic solid waste: A state of art review and future applications, *Compos. Part B Eng.*, 2017, **115**, 409–422.

21 Grand View Research, Plastic Market Size, Growth & Trends Report, 2021-2028, *Gd. View Res.*, 2021, 230.

22 J. C. Prata, A. L. P. Silva, T. R. Walker, A. C. Duarte and T. Rocha-Santos, COVID-19 Pandemic Repercussions on the Use and Management of Plastics, *Environ. Sci. Technol.*, 2020, **54**, 7760–7765.

23 ExxonMobil boosts production of raw materials for medical masks, gowns and hand sanitizer | ExxonMobil, https://corporate.exxonmobil.com/News/Newsroom/News-releases/2020/0415_ExxonMobil-boosts-production-of-raw-materials-for-medical-masks-

and-gowns-and-hand-sanitizer, (accessed 4 February 2022).

24 M. Saberian, J. Li, S. Kilmartin-Lynch and M. Boroujeni, Repurposing of COVID-19 single-use face masks for pavements base/subbase, *Sci. Total Environ.*, 2021, **769**, 145527.

25 D. Hantoko, X. Li, A. Pariatamby, K. Yoshikawa, M. Horttanainen and M. Yan, Challenges and practices on waste management and disposal during COVID-19 pandemic, *J. Environ. Manage.*, 2021, **286**, 112140.

26 N. U. Benson, D. E. Bassey and T. Palanisami, COVID pollution: impact of COVID-19 pandemic on global plastic waste footprint, *Heliyon*, 2021, **7**, 06343.

27 Ellen MacArthur Foundation, in *Ellen MacArthur Foundation*, 2017, p. 68.

28 'More Masks Than Jellyfish': The devastating impact of PPE on marine life, https://www.openaccessgovernment.org/more-masks-than-jellyfish-ppe-marine-life/105123/, (accessed 4 February 2022).

29 N. Voulvoulis, R. Kirkman, T. Giakoumis, P. Metivier, C. Kyle and V. Midgle, Examining Material Evidence - The Carbon Footprint, 2020, 1–15.

30 D. Amienyo, H. Gujba, H. Stichnothe and A. Azapagic, Life cycle environmental impacts of carbonated soft drinks, *Int. J. Life Cycle Assess.*, 2013, **18**, 77–92.

31 GOV.UK, Circular Economy Package policy statement - GOV.UK, https://www.gov.uk/government/publications/circular-economy-package-policy-statement/circular-economy-package-policy-statement, (accessed 27 January 2021).

32 F. & R. A. Department for Environment, Circular economy measures drive forward ambitious plans for waste, https://www.gov.uk/government/news/circular-economy-measures-drive-forward-ambitious-plans-for-waste, (accessed 2 August 2021).

33 E. Watkins and J.-P. Schweitzer, Moving Towards a Circular Economy for Plastics in the Eu By 2030, *Inst. Eur. Environ. Policy*, 2019, 4–16.

34 New study reveals 93.5% of PET bottles were recycled in Germany last year, https://www.packaging-gateway.com/news/new-study-reveals-935-pet-bottles-were-recycled-last-year-in-germany-5691549/, (accessed 5 August 2021).

35 V. Shanmugam, O. Das, R. E. Neisiany, K. Babu, S. Singh, M. S. Hedenqvist, F. Berto and S. Ramakrishna, Polymer Recycling in Additive Manufacturing: an Opportunity for the Circular Economy, *Mater. Circ. Econ.*, 2020, **2**, 1–11.

36 Plastics and packaging laws in France| CMS Expert Guide, https://cms.law/en/int/expert-guides/plastics-and-packaging-laws/france, (accessed 5 August 2021).

37 E. Watkins, S. Gionfra, J.-P. Schweitzer, M. Pantzar, C. Janssens and P. ten Brink, EPR in the EU Plastics Strategy and the Circular Economy: A focus on plastic packaging, *Inst. Eur. Environ. Policy*, 2017, 52.

38 A. A. Bull, Oil consumption, https://www.bpf.co.uk/press/Oil_Consumption.aspx, (accessed 3 March 2022).

39 A. L. Andrady and M. A. Neal, Applications and societal benefits of plastics, *Philos. Trans. R. Soc. B Biol. Sci.*, 2009, **364**, 1977–1984.

40 Lidl, Plastic strategy - Styleguide, https://ec.europa.eu/environment/strategy/plastics-strategy_en, (accessed 30 September 2021).

41 V. Kouloumpis, R. S. Pell, M. E. Correa-Cano and X. Yan, Potential trade-offs between eliminating plastics and mitigating climate change: An LCA perspective on Polyethylene Terephthalate (PET) bottles in Cornwall, *Sci. Total Environ.*, 2020, **727**, 138681.

42 D. B. Malpass, *Introduction to Polymers of Ethylene*, John Wiley & Sons, Ltd, 2010.

43 A. J. Peacock, in *Journal of Macromolecular Science - Polymer Reviews*, CRC Press, 2001, vol. 41, pp. 285–323.

44 J. M. Restrepo-Flórez, A. Bassi and M. R. Thompson, Microbial degradation and deterioration of polyethylene - A review, *Int. Biodeterior. Biodegrad.*, 2014, **88**, 83–90.

45 A. R. White, in *Packaging Technology: Fundamentals, Materials and Processes*, Woodhead Publishing, 2012, pp. 395–407.

46 S. Ronca, in *Brydson's Plastics Materials: Eighth Edition*, Butterworth-Heinemann, 2017, pp. 247–278.

47 E. Redzic, T. Garoff, C. C. Mardare, M. List, G. Hesser, L. Mayrhofer, A. W. Hassel and C. Paulik, Heterogeneous Ziegler–Natta catalysts with various sizes of MgCl2 crystallites: synthesis and characterization, *Iran. Polym. J. (English Ed.*, 2016, **25**, 321–337.

48 W. Kaminsky and A. Laban, Metallocene catalysis, *Appl. Catal. A Gen.*, 2001, **222**, 47–61.

49 J. Huang and G. L. Rempel, Ziegler-Natta catalysts for olefin polymerization: Mechanistic insights from metallocene systems, *Prog. Polym. Sci.*, 1995, **20**, 459–526.

50 C. E. Carraher Jr., in *Carraher's Polymer Chemistry*, Third Edit., 2020, pp. 21–44.

51 L. Petitjean, D. Pattou and M. F. Ruiz-López, Theoretical study of the mechanisms of ethylene polymerization with metallocene-type catalysts, *J. Phys. Chem. B*, 1999, **103**, 27–35.

52 H. G. Alt and A. Köppl, Effect of the nature of metallocene complexes of group IV metals on their performance in catalytic ethylene and propylene polymerization, *Chem. Rev.*, 2000, **100**, 1205–1221.

53 H. G. Alt, The heterogenization of homogeneous metallocene catalysts for olefin polymerization, *J. Chem. Soc. - Dalt. Trans.*, 1999, 1703–1709.

54 M. P. McDaniel, A review of the Phillips Chromium Catalyst for Ethylene Polymerization, *Handb. Transit. Met. Polym. Catal. Second Ed.*, 2018, 401–571.

55 J. Vega, M. Aguilar, J. Peón, D. Pastor and J. Martínez-Salazar, *Effect of long chain branching on linear-viscoelastic melt properties of polyolefins*, European Polymer Federation, 2002, vol. 2.

56 Molgroup, *Product Catalogue - High Density Polyethylene*, 2018.

57 H. R. Sailors and J. P. Hogan, History of Polyolefins, *J. Macromol. Sci. Part A - Chem.*, 1981, **15**, 1377–1402.

58 J. Hopewell, R. Dvorak and E. Kosior, Plastics recycling: Challenges and opportunities, *Philos. Trans. R. Soc. B Biol. Sci.*, 2009, **364**, 2115–2126.

59 J. S. Higgins, J. E. G. Lipson and R. P. White, A simple approach to polymer mixture miscibility, *Philos. Trans. R. Soc. A Math. Phys. Eng. Sci.*, 2010, **368**, 1009–1025.

60 A. Graziano, S. Jaffer and M. Sain, Review on modification strategies of polyethylene/polypropylene immiscible thermoplastic polymer blends for enhancing their mechanical behavior, *J. Elastomers Plast.*, 2019, **51**, 291–336.

61 N. P. Cheremisinoff, *Condensed encyclopedia of polymer engineering terms*, Butterworth-Heinemann, 2001, vol. 39.

62 D. Mangaraj, in *Comprehensive Polymer Science and Supplements*, Pergamon, 1989, pp. 605–667.

63 John Goff and Tony Whelan, *The Dynisco Extrusion Processors Handbook*, Dynisco, 2nd edn., 2013.

64 Dynisco, An Introduction to Single Screw Extrusion, https://www.azom.com/article.aspx?ArticleID=13566, (accessed 17 October 2021).

65 D. Acierno, L. Di Maio and C. C. Ammirati, Film casting of polyethylene terephthalate: Experiments and model comparisons, *Polym. Eng. Sci.*, 2000, **40**, 108–117.

66 J. L. White and H. B. Dee, Flow visualization for injection molding of polyethylene and polystyrene melts, *Polym. Eng. Sci.*, 1974, **14**, 212–222.

67 C. Yu, J. Liu, X. Tang, X. Shen and S. Liu, in *RSC Advances*, Royal Society of Chemistry, 2017, vol. 7, pp. 11979–11986.

68 S. Godavarti and M. V. Karwe, Determination of specific mechanical energy distribution on a twin-screw extruder, *J. Agric. Eng. Res.*, 1997, **67**, 277–287.

69 A. Schweighuber, A. Felgel-Farnholz, T. Bögl, J. Fischer and W. Buchberger, Investigations on the influence of multiple extrusion on the degradation of polyolefins, *Polym. Degrad. Stab.*, 2021, **192**, 109689.

70 M. J. Abad, A. Ares, L. Barral, J. Cano, F. J. Díez, S. García-Garabal, J. López and C. Ramírez, Effects of a mixture of stabilizers on the structure and mechanical properties of polyethylene during reprocessing, *J. Appl. Polym. Sci.*, 2004, **92**, 3910–3916.

71 J. Vera-Sorroche, A. L. Kelly, E. C. Brown, T. Gough, C. Abeykoon, P. D. Coates, J. Deng, K. Li, E. Harkin-Jones and M. Price, The effect of melt viscosity on thermal efficiency for single screw extrusion of HDPE, *Chem. Eng. Res. Des.*, 2014, **92**, 2404–2412.

72 I. I. Salakhov, N. M. Shaidullin, A. E. Chalykh, M. A. Matsko, A. V. Shapagin, A. Z. Batyrshin, G. A. Shandryuk and I. E. Nifant'ev, Low-temperature mechanical properties of high-density and low-density polyethylene and their blends, *Polymers (Basel).*, 2021, **13**, 1821.

73 Intertek, Melt Flow Rate ASTM D 1238, ISO 1133, http://www.intertek.com/polymers/testlopedia/melt-flow-rate-astm-d1238/, (accessed 3 March 2022).

74 T. Bremner, A. Rudin and D. G. Cook, Melt flow index values and molecular weight distributions of commercial thermoplastics, *J. Appl. Polym. Sci.*, 1990, **41**, 1617–1627.

75 A. J. Franck, Understanding Rheology of Thermosets, *TA Instruments*, 2004, **AAN015**, 14.

76 T. C. B. McLeish, Tube theory of entangled polymer dynamics, *Adv. Phys.*, 2002, **51**, 1379–1527.

77 G. W. Kamykowski, in *Handbook of Transition Metal Polymerization Catalysts*, John Wiley & Sons, Ltd, 2010, pp. 563–566.

78 W. Gleissle and B. Hochstein, Validity of the Cox–Merz rule for concentrated suspensions, *J. Rheol. (N. Y. N. Y).*, 2003, **47**, 897–910.

79 R. Rathner, W. Roland, H. Albrecht, F. Ruemer and J. Miethlinger, Applicability of the Cox-Merz Rule to High-Density Polyethylene Materials with Various Molecular Masses, *Polymers (Basel).*

80 J. R. Wagner, E. M. Mount and H. F. Giles, in *Extrusion: The Definitive Processing Guide and Handbook: Second Edition*, William Andrew Publishing, 2013, pp. 1–620.

81 E. Garofalo, P. Scarfato, L. Di Maio, A. Protopapa and L. Incarnato, Zeolites as effective desiccants to solve hygroscopicity issue of post-consumer mixed recycled polyolefins, *J. Clean. Prod.*, 2021, **295**, 126379.

82 A. Cabanes, M. Strangl, E. Ortner, A. Fullana and A. Buettner, Odorant composition of post-consumer LDPE bags originating from different collection systems, *Waste Manag.*, 2020, **104**, 228–238.

83 E. Epacher, J. Tolvéth, C. Kröhnke and B. Pukánszky, Processing stability of high density polyethylene: Effect of adsorbed and dissolved oxygen, *Polymer (Guildf).*, 2000, **41**, 8401–8408.

84 P. G. Lafleur and B. Vergnes, in *Polymer Extrusion*, Wiley Blackwell, 2014, vol. 1, pp. 1–337.

85 F. Gugumus, Thermooxidative degradation of polyolefins in the solid state. Part 2: Homogeneous and heterogeneous aspects of thermal oxidation, *Polym. Degrad. Stab.*, 1996, **52**, 145–157.

86 J. Dostál, V. Kašpárková, M. Zatloukal, J. Muras and L. Šimek, Influence of the repeated extrusion on the degradation of polyethylene. Structural changes in low density polyethylene, *Eur. Polym. J.*, 2008, **44**, 2652–2658.

87 P. Gijsman, M. Kroon and M. Van Oorschot, The role of peroxides in the thermooxidative degradation of polypropylene, *Polym. Degrad. Stab.*, 1996, **51**, 3–13.

88 P. Gijsman, G. Hensen and M. Mak, Thermal initiation of the oxidation of thermoplastic polymers (Polyamides, Polyesters and UHMwPE), *Polym. Degrad. Stab.*, 2021, **183**, 109452.

89 H. Zweifel, R. D. Maier and M. Schiller, in *Additives for Polymers*, 6th edn., 1991, vol. 1991, p.

15.

90 P. Gijsman, *Review on the thermo-oxidative degradation of polymers during processing and in service*, European Polymer Federation, 2008, vol. 8.

91 L. A. Pinheiro, M. A. Chinelatto and S. V. Canevarolo, The role of chain scission and chain branching in high density polyethylene during thermo-mechanical degradation, *Polym. Degrad. Stab.*, 2004, **86**, 445–453.

92 T. Kealy, Rheological analysis of the degradation of HDPE during consecutive processing steps and for different processing conditions, *J. Appl. Polym. Sci.*, 2009, **112**, 639–648.

93 S. Moss and H. Zweifel, Degradation and stabilization of high density polyethylene during multiple extrusions, *Polym. Degrad. Stab.*, 1989, **25**, 217–245.

94 S. Luzuriaga, J. Kovářová and I. Fortelný, Degradation of pre-aged polymers exposed to simulated recycling: Properties and thermal stability, *Polym. Degrad. Stab.*, 2006, **91**, 1226–1232.

95 M. Altan, M. E. Yurci and N. Nugay, *Residual stresses determination in injection molded virgin and recycled HDPE blends: Mechanical properties and morphology*, De Gruyter, 2008, vol. 8.

96 E. Epacher, J. Tolvéth, K. Stoll and B. Pukánszky, Two-step degradation of high-density polyethylene during multiple extrusion, *J. Appl. Polym. Sci.*, 1999, **74**, 1596–1605.

97 S. Apone, R. Bongiovanni, M. Braglia, D. Scalia and A. Priola, Effects of thermomechanical treatments on HDPE used for TLC ducts, *Polym. Test.*, 2003, **22**, 275–280.

98 P. Oblak, J. Gonzalez-Gutierrez, B. Zupančič, A. Aulova and I. Emri, Processability and mechanical properties of extensively recycled high density polyethylene, *Polym. Degrad. Stab.*, 2015, **114**, 133–145.

99 M. K. Loultcheva, M. Proietto, N. Jilov and F. P. L. Mantia, Recycling of high density polyethylene containers, *Polym. Degrad. Stab.*, 1997, **57**, 77–81.

100 J. N. Hahladakis, C. A. Velis, R. Weber, E. Iacovidou and P. Purnell, An overview of chemical additives present in plastics: Migration, release, fate and environmental impact during their use, disposal and recycling, *J. Hazard. Mater.*, 2018, **344**, 179–199.

101 R. D. Deanin, Additives in plastics, *Environ. Health Perspect.*, 1975, **vol.11**, 35–39.

102 E. Hansen, N. H. Nilsson, D. Lithner and C. Lassen, in *Hazardous substances in plastic*

materials, 2013, p. 148.

103 H. Moustafa, C. Guizani and A. Dufresne, Sustainable biodegradable coffee grounds filler and its effect on the hydrophobicity, mechanical and thermal properties of biodegradable PBAT composites, *J. Appl. Polym. Sci.*, 2017, **134**, 44498.

104 MA Business Ltd, BASF launches IrgaCycle additive solutions for mechanical recycling of plastics, *Angew. Chemie Int. Ed. 6(11), 951–952.*, 2021, **13**, 1–2.

105 A. Chamas, H. Moon, J. Zheng, Y. Qiu, T. Tabassum, J. H. Jang, M. Abu-Omar, S. L. Scott and S. Suh, Degradation Rates of Plastics in the Environment, *ACS Sustain. Chem. Eng.*, 2020, **8**, 3494–3511.

106 C. Maier and T. Calafut, in *Polypropylene*, William Andrew Publishing, 1998, pp. 27–47.

107 M. Tolinski, in *Additives for Polyolefins*, Elsevier, 2015, pp. 183–189.

108 S. F. Laermer and P. F. Zambetti, Alpha-tocopherol (vitamin E)—the natural antioxidant for polyolefins, *J. Plast. Film Sheeting*, 1992, **8**, 228–248.

109 B. Kirschweng, D. Tátraaljai, E. Földes and B. Pukánszky, Natural antioxidants as stabilizers for polymers, *Polym. Degrad. Stab.*, 2017, **145**, 25–40.

110 K. J. Olejar, S. Ray and P. A. Kilmartin, Enhanced antioxidant activity of polyolefin films integrated with grape tannins, *J. Sci. Food Agric.*, 2016, **96**, 2825–2831.

111 K. Schwetlick, Mechanisms op antioxidant action op organic phosphorus compounds, *Pure Appl. Chem.*, 1983, **55**, 1629–1636.

112 E. A. Coleman, Plastics Additives, *Appl. Plast. Eng. Handb. Process. Mater. Appl. Second Ed.*, 2017, 489–500.

113 M. Skocaj, M. Filipic, J. Petkovic and S. Novak, Titanium dioxide in our everyday life; Is it safe?, *Radiol. Oncol.*, 2011, **45**, 227–247.

114 D. Rivin, in *Handbook of Environmental Chemistry*, Springer, Dordrecht, 1986, vol. 3, pp. 101–158.

115 M. J. Abad, A. Ares, L. Barral, J. Cano, F. J. Díez, S. García-Garabal, J. López and C. Ramírez, Effects of a mixture of stabilizers on the structure and mechanical properties of polyethylene during reprocessing, *J. Appl. Polym. Sci.*, 2004, **92**, 3910–3916.

116 F. R. Beltrán, C. Infante, M. U. de la Orden and J. Martínez Urreaga, Mechanical recycling of

poly(lactic acid): Evaluation of a chain extender and a peroxide as additives for upgrading the recycled plastic, *J. Clean. Prod.*, 2019, **219**, 46–56.

117 T. Corrales, F. Catalina, C. Peinado, N. S. Allen and E. Fontan, Photooxidative and thermal degradation of polyethylenes: Interrelationship by chemiluminescence, thermal gravimetric analysis and FTIR data, *J. Photochem. Photobiol. A Chem.*, 2002, **147**, 213–224.

118 ISO, *ISO 527-1:2019 Determination of tensile properties — Part 1: General principles*, 2019, vol. 2019.

119 C. J. Kuo and W. L. Lan, in *Advances in Filament Yarn Spinning of Textiles and Polymers*, Elsevier Ltd., 2014, pp. 100–112.

120 A. Dutta, On viscosity - melt flow index relationship, *Rheol. Acta*, 1984, **23**, 565–569.

121 E. Ostertagová, Modelling using polynomial regression, *Procedia Eng.*, 2012, **48**, 500–506.

122 A. V. Shenoy and D. R. Saini, Melt flow index: More than just a quality control rheological parameter. Part II, *Adv. Polym. Technol.*, 1986, **6**, 125–145.

123 S. L. Morelly and N. J. Alvarez, Characterizing long-chain branching in commercial HDPE samples via linear viscoelasticity and extensional rheology, *Rheol. Acta*, 2020, **59**, 797–807.

124 US7422786B2 - Collation shrink - Google Patents, https://patents.google.com/patent/US7422786B2/en, (accessed 24 February 2022).

125 WO2017184234A1 - Polyethylene sheets - Google Patents, https://patents.google.com/patent/WO2017184234A1/en, (accessed 24 February 2022).

126 M. Amjadi and A. Fatemi, *Tensile behavior of high-density polyethylene including the effects of processing technique, thickness, temperature, and strain rate*, Multidisciplinary Digital Publishing Institute (MDPI), 2020, vol. 12.

127 J. J. Cheng, J. A. Alvarado-Contreras, M. A. Polak and A. Penlidis, Chain Entanglements and Mechanical Behavior of High Density Polyethylene, , DOI:10.1115/1.4000220.

128 J. V. Gulmine, P. R. Janissek, H. M. Heise and L. Akcelrud, in *Polymer Testing*, 2002, vol. 21, pp. 557–563.

129 H. Hassani, Z. Akbaripanah, R. Rashedi and N. Feizi, A new method for investigation of short-chain branching distribution in polyethylene by combined use of FTIR and TREF, *J. Indian Chem. Soc.*, 2020, **97**, 887–893.

130 J. Almond, P. Sugumaar, M. N. Wenzel, G. Hill and C. Wallis, Determination of the carbonyl index of polyethylene and polypropylene using specified area under band methodology with ATR-FTIR spectroscopy, *E-Polymers*, 2020, **20**, 369–381.

131 J. Kim, K. Choi and D. S. Chung, Sample preparation for capillary electrophoretic applications, *Compr. Sampl. Sample Prep.*, 2012, **3**, 701–721.

132 M. Arias, I. Penichet, F. Ysambertt, R. Bauza, M. Zougagh and Á. Ríos, Fast supercritical fluid extraction of low- and high-density polyethylene additives: Comparison with conventional reflux and automatic Soxhlet extraction, *J. Supercrit. Fluids*, 2009, **50**, 22–28.

133 H. J. Vandenburg, A. A. Clifford, K. D. Bartle, J. Carroll, I. Newton, L. M. Garden, J. R. Dean and C. T. Costley, Analytical extraction of additives from polymers, *Analyst*, 1997, **122**, 101R-116R.

134 J. Lehotay, J. Daněček, O. Líška, J. Leško and E. Brandšteterová, Analytical study of the additives system in polyethylene, *J. Appl. Polym. Sci.*, 1980, **25**, 1943–1950.

135 J. F. Schabron, Determination Of Polyolefin Additives By Normal-Phase High Performance Liquid Chromatography Following Soxhlet Extraction, *J. Liq. Chromatogr.*, 1982, **5**, 1269–1276.

136 A. Patil, K. S. Choudhari, V. Prabhu, V. K. Unnikrishnan, S. Bhat, K. M. Pai, V. B. Kartha and C. Santhosh, Highly Sensitive High Performance Liquid Chromatography-Laser Induced Fluorescence for Proteomics Applications, *ISRN Spectrosc.*, 2012, **2012**, 1–9.

137 H. Junghare, M. Hamjade, C. K. Patil, S. B. Girase and M. M. Lele, *A Review on Cryogenic Grinding*, 2020.

138 J. Murphy, *Additives for Plastics Handbook*, Elsevier, 2nd edn., 2001.

139 J. Pospíšil, W. D. Habicher, J. Pilař, S. Nešpůrek, J. Kuthan, G. O. Piringer and H. Zweifel, Discoloration of polymers by phenolic antioxidants, *Polym. Degrad. Stab.*, 2002, **77**, 531–538.

140 P. P. Klemchuk and P. L. Horng, Transformation products of hindered phenolic antioxidants and colour development in polyolefins, *Polym. Degrad. Stab.*, 1991, **34**, 333–346.

141 C. Li, J. Wang, M. Ning and H. Zhang, Synthesis and antioxidant activities in polyolefin of dendritic antioxidants with hindered phenolic groups and tertiary amine, *J. Appl. Polym. Sci.*, 2012, **124**, 4127–4135.

142 T. Kikuchi, Y. Ohtake and K. Tanaka, Discoloration phenomenon induced by the combination of phenolic antioxidants & hindered amine light stabilisers, *Int. Polym. Sci. Technol.*, 2013, **40**, 283–288.

143 G. Pastorelli, C. Cucci, O. Garcia, G. Piantanida, A. Elnaggar, M. Cassar and M. Strlič, Environmentally induced colour change during natural degradation of selected polymers, *Polym. Degrad. Stab.*, 2014, **107**, 198–209.

144 ASTM, Standard Practice for Calculating Yellowness and Whiteness Indices from Instrumentally Measured Color Coordinates, http://www.astm.org/cgi-bin/resolver.cgi?E313-15e1, (accessed 9 October 2021).

145 TA Instruments, *Application Of Rheology Of Polymers*, 2004.

146 X. Xu, J. Chen and L. An, Shear thinning behavior of linear polymer melts under shear flow via nonequilibrium molecular dynamics, *J. Chem. Phys.*, 2014, **140**, 174902.

147 A. Jabbarzadeh, J. D. Atkinson and R. I. Tanner, Effect of molecular shape on rheological properties in molecular dynamics simulation of star, H, comb, and linear polymer melts, *Macromolecules*, 2003, **36**, 5020–5031.

148 M. Kontopoulou, in *Applied Polymer Rheology: Polymeric Fluids with Industrial Applications*, Wiley, 2011, p. 354.

149 L. D. T. Topoleski, in *Kinesiology: The Mechanics and Pathomechanics of Human Movement: Second Edition*, Academic Press, 2013, pp. 21–35.

150 W. N. Dos Santos, J. A. De Sousa and R. Gregorio, Thermal conductivity behaviour of polymers around glass transition and crystalline melting temperatures, *Polym. Test.*, 2013, **32**, 987–994.

151 K. Balani, V. Verma, A. Agarwal and R. Narayan, in *Biosurfaces*, John Wiley & Sons, Ltd, 2015, pp. 329–344.

152 C. Rouillon, P. O. Bussiere, E. Desnoux, S. Collin, C. Vial, S. Therias and J. L. Gardette, Is carbonyl index a quantitative probe to monitor polypropylene photodegradation?, *Polym. Degrad. Stab.*, 2016, **128**, 200–208.

7 Appendices

7.1 Rheology

7.1.1 Viscosity Measurements of Recycling Cycles of ExxonMobil grades (Magnified)

Complex Viscosity with respect to extrusion cycles at 25 rad/s. HMA018 (Blue) HMA016 (Orange) HMA014 (Black). HMA014 shows an overall increase in viscosity with extrusion cycles, yet the fluctuations for HMA016 and HMA018 may indicate simultaneous chain scission and branching.

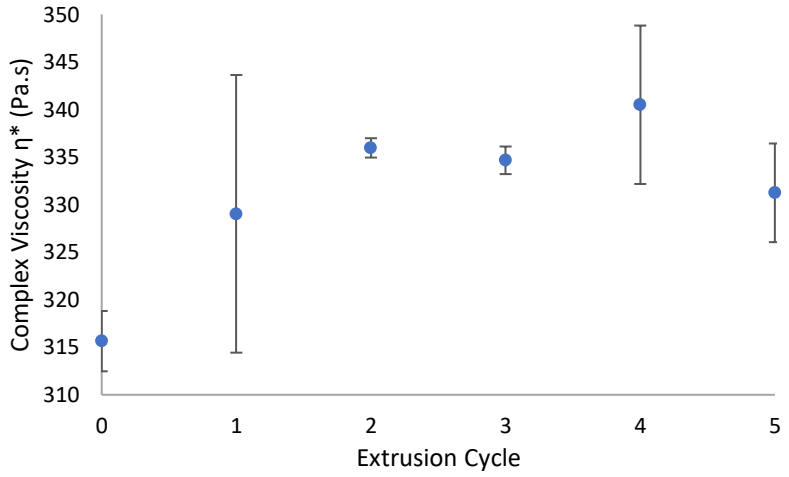

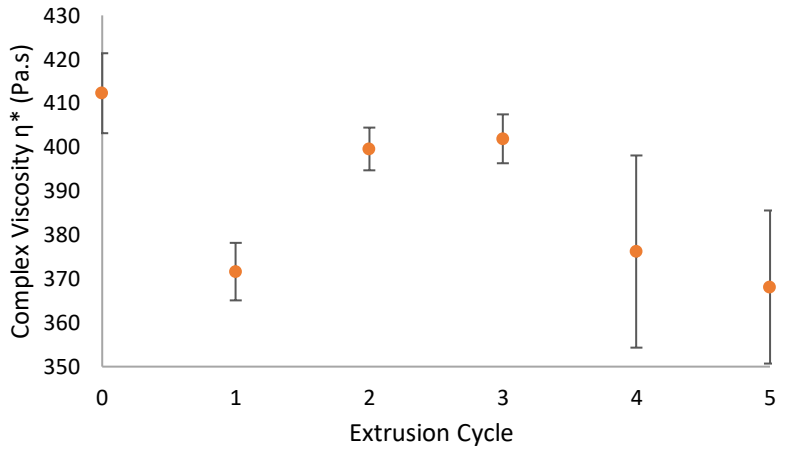

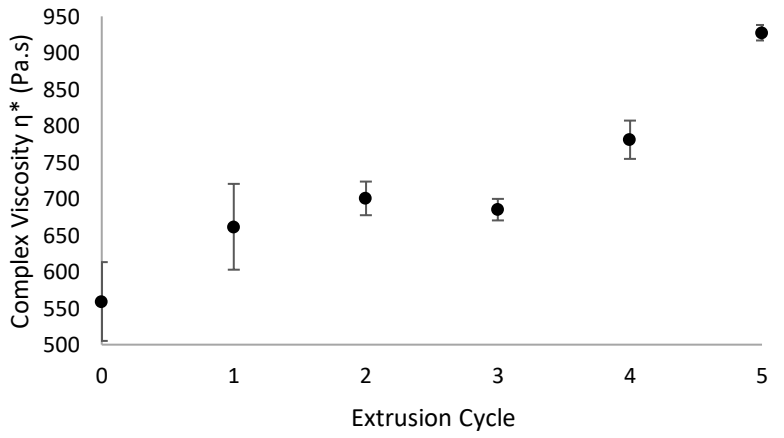

7.1.2 Viscosity Measurements of Virgin HDPE Grades at 25 rad/s

Complex viscosity (η*) measured at 25 rad/s and MFI of different HDPE grades. At 0.1 rad/s the correlation between MFI and η* is more linear, where η* increases with decreasing MFI. However, at 25 rad/s this trend is disrupted as shown below.

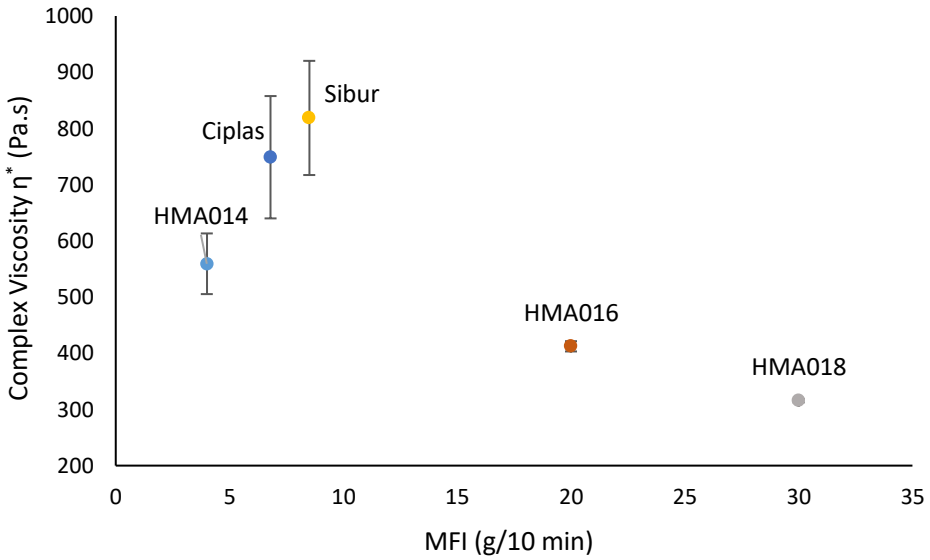

Correlation between complex viscosity, η*, at 25 rad/s and crystallinity of different HDPE grades (R^2 = 0.50). The η* increases with % crystallinity, however Ciplas does not fit the trend.